JACS
JOURNAL OF THE AMERICAN CHEMICAL SOCIETY
Article
pubs.acs.org/JACS

Diastereomeric Spirooxindoles as Highly Potent and Efficacious MDM2 Inhibitors

Yujun Zhao,[†] Liu Liu,[†] Wei Sun,[†] Jianfeng Lu,[†] Donna McEachern,[†] Xiaoqin, Li,[‡] Shanghai Yu,[†] Denzil Bernard,[†] Philippe Ochsenbein,[§] Vincent Ferey,[§] Jean-Christophe Carry,[∥] Jeffrey R. Deschamps,[⊥] Duxin Sun,[‡] and Shaomeng Wang*[,†]

[†]Comprehensive Cancer Center and Departments of Internal Medicine, Pharmacology and Medicinal Chemistry, and [‡]Life Sciences Institute, University of Michigan, 1500 East Medical Center Drive, Ann Arbor, Michigan 48109, United States

[§]Sanofi Research & Development, Montpellier, France

[∥]Sanofi Research & Development, Vitry-sur-Seine, France

[⊥]Naval Research Laboratory, Code 6930, 4555 Overlook Avenue, Washington, D.C. 20375, United States

Supporting Information

ABSTRACT: Small-molecule inhibitors that block the MDM2-p53 protein−protein interaction (MDM2 inhibitors) are being intensely pursued as a new therapeutic strategy for cancer treatment. We previously published a series of spirooxindole-containing compounds as a new class of MDM2 small-molecule inhibitors. We report herein a reversible ring-opening-cyclization reaction for some of these spirooxindoles, which affords four diastereomers from a single compound. Our biochemical binding data showed that the stereochemistry in this class of compounds has a major effect on their binding affinities to MDM2, with >100-fold difference between the most potent and the least potent stereoisomers. Our study has led to the identification of a set of highly potent MDM2 inhibitors with a stereochemistry that is different from that of our previously reported compounds. The most potent compound (**MI-888**) binds to MDM2 with a K_i value of 0.44 nM and achieves complete and long-lasting tumor regression in an animal model of human cancer.

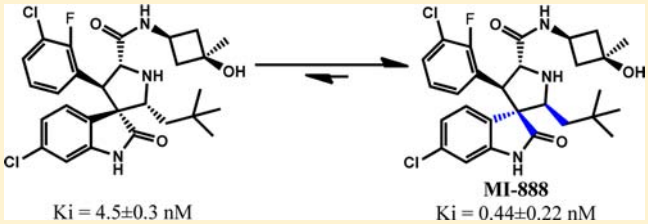

INTRODUCTION

Compounds containing a spirocyclic oxindole-pyrrolidine ring (spirooxindole) system have recently attracted significant attention because of their unique structure and broad biological activities (Figure 1).[1] For example, the natural product spirotryprostatin A is a cell cycle regulator,[2] while pteropodine is a modulator of muscarinic M_1 and 5-HT_2 receptors.[3]

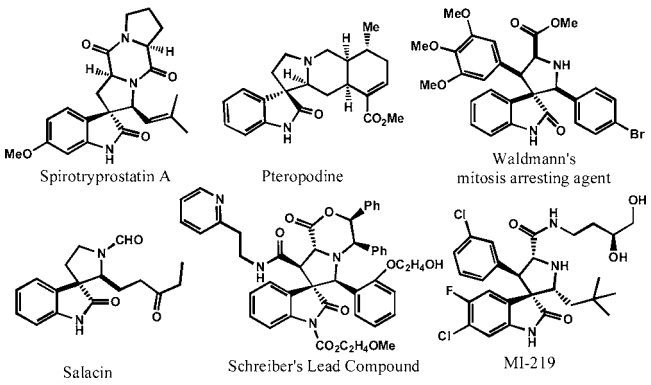

Figure 1. Examples of spirooxindole-containing compounds with interesting biological activities.

Additionally, spirooxindole-containing compounds have been reported as actin polymerization inhibitors,[4] and as inhibitors of tubulin polymerization.[5]

We previously reported sprirooxindole-containing compounds that are potent and specific small-molecule inhibitors that block the MDM2-p53 protein−protein interaction.[6] For example, compound MI-219 (Figure 1) binds to MDM2 with low nanomolar affinity, effectively blocks the MDM2-p53 protein−protein interaction in cells, reactivates p53 in tumor cells with wild-type p53 *in vitro* and *in vivo*, and strongly inhibits tumor growth in animal models of human cancer.[6b] Our data thus suggested that modifications of spirooxindole-containing compounds may lead to a highly promising MDM2 inhibitor for the treatment of human cancer by reactivation of the powerful tumor suppressor function of p53.

Our spirooxindole-containing MDM2 inhibitors were synthesized using an efficient 1,3-dipolar cycloaddition reaction (Scheme 1).[6d] Compound **1a** was obtained in high purity and was found to be relatively stable in aprotic solvents such as CH_2Cl_2, THF, EtOAc, and DMSO. Stereochemistry was assigned to compound **1a** and its analogues, including MI-

Received: December 22, 2012
Published: May 3, 2013

   dx.doi.org/10.1021/ja3125417 | *J. Am. Chem. Soc.* 2013, 135, 7223−7234

Scheme 1. Synthesis and Chemical Structures of Our Previously Reported MDM2 Inhibitors

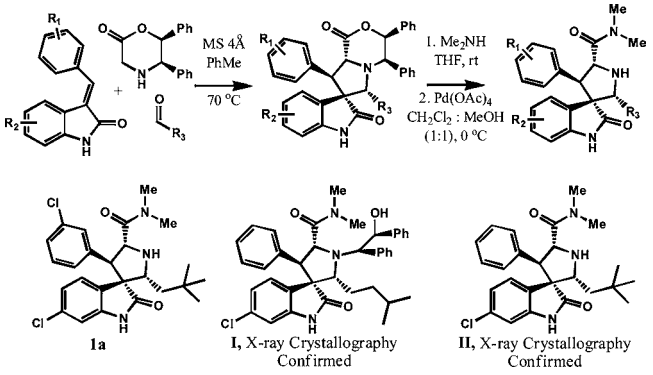

219, using the X-ray crystal structures of the key intermediate **I** and of compound **II** (Figure 1 and Scheme 1).[7] However, when a pure sample of **1a** was treated with MeOH or CH_3CN/H_2O, up to four peaks, all with the same molecular weight, were observed by analytical HPLC (Supporting Information, SI). Isolation and purification of the fractions from compound **1a** and subsequent analysis by ^1H, DEPT 135, and ^{13}C NMR showed that individual components possess the same number of protons, CH, CH_2, CH_3, and quaternary carbons. The data suggested that these individual peaks represent different isomers or stereoisomers.

Based upon these initial observations and on our subsequent investigations, we hypothesized that reversible ring-opening and cyclization of the pyrrolidine ring takes place in some of these compounds. A cascade reaction of this type can generate four possible diastereomers from one single stereoisomer, as shown in Table 1. Although reversible ring-opening-cyclization has been previously observed for certain spirooxindole-

Table 1. Isomerization of Selected Spirooxindole-Containing Compounds[a]

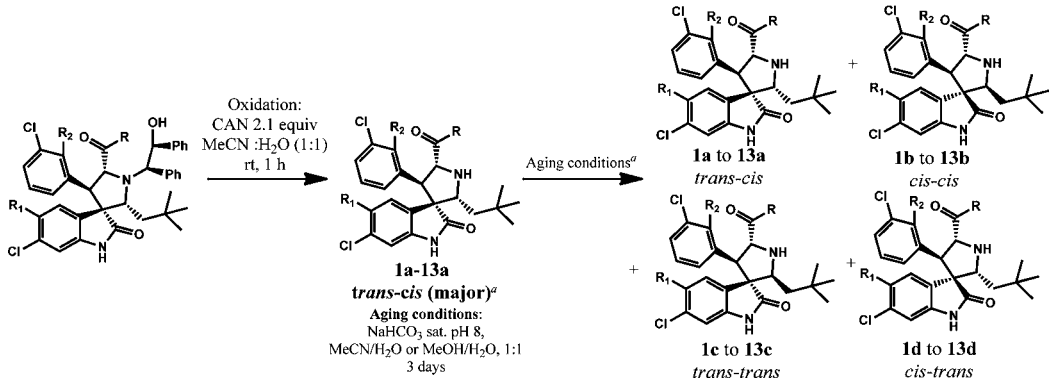

Entry	Compounds (a-d)	R_1	R_2	R	Yield[b] (%)	Ratio after Oxidation a:b: (c+d)[c]	Ratio after Aging a:b: (c+d)[c,d]
1	**1**	H	H	NMe_2	50[e]	95:2:3	6:71:24
2	**2**	H	H	NHMe	61	87:5:8	3:71:26
3	**3**	H	F	NMe_2	57	75:19:6	35:46:19
4	**4**	H	F	NHMe	84	67:2:31	9:79:12
5	**5**	H	F	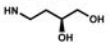	86	88:2:10	1:80:19
6	**6**	H	F	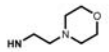	79	89:10:1	12:61:27
7	**7**	H	F	OEt	74	89:6:3	44:50:6
8	**8**[f]	H	F	OH	25[g]	___	41:34:25[h]
9[a]	**9**	H	F	NH_2	56	0:44:56	0:96:4
10	**10**	F	H	NMe_2	60	56:25:19	10:71:19[i] 2:88:8
11[a]	**11**	F	H	NHMe	87	19:52:27	1:74:25
12	**12**	F	H	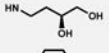	81	30:32:38	3:58:37
13[a]	**13**	F	H	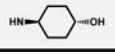	50	15:67:18	2:74:24

[a]In cases of **9**, **11**, and **13**, the *cis*–*cis* isomers were obtained as the predominant products of ceric ammonium nitrate oxidation without aging (equilibrium in CH_3CN and H_2O at pH 8 for 3 days). [b]Isolated yield after flash column chromatography. [c]Ratio determined by HPLC analysis; assignments were not made for **c** and **d**. [d]The combined yield of **a** to **d** in the aging step was determined from the yield in the oxidation step. [e]Yield after HPLC separation. [f]Compound **8a**–**8d** was obtained from the hydrolysis by LiOH-THF-H_2O of **7a**. [g]Hydrolysis yield. [h]Starting from pure **8a**. [i]Ratio after crude product was allowed to stand in MeOH for 2 h.

dx.doi.org/10.1021/ja3125417 | J. Am. Chem. Soc. 2013, 135, 7223–7234

containing alkaloids,[8] no detailed investigation has been reported.

We herein report our detailed investigation of the isomerization of selected spirooxindole-containing compounds. Our biochemical binding data showed that the stereochemistry in this class of compounds has a major effect on their binding affinities to MDM2; with >100-fold difference between the most potent and the least potent stereoisomers. Importantly, our investigation has led to the identification of a set of highly potent MDM2 inhibitors with a stereochemistry that is different from that of our previously reported compounds.[6] One such compound is capable of achieving complete and long-lasting tumor regression in an animal model of human cancer.

RESULTS AND DISCUSSION

We first investigated the isomerization reaction for selected spirooxindole-containing compounds (entries 1−13, Table 1). The *trans*−*cis* isomers, **1a**-**7a**, were obtained as major products (67−95%) after ceric ammonium nitrate (CAN) oxidation (Table 1, entries 1−7).

However, treatment of the oxidation reaction products (entries 1−7) with CH_3CN and H_2O at pH 8 for 3 days (aging) produced a mixture of four isomers with the *cis*−*cis* isomers (**1b** to **7b**) as the major components. Hydrolysis of **7a** yielded a mixture of four isomers **8a**−**8d**. Interestingly, for entry 9, after CAN oxidation, a mixture of **9b**−**9d** was obtained without detectable amount of **9a**. Although **10a** constituted 56% after oxidation, this isomer rapidly decreased to 10% within 2 h in MeOH. When R_1 = F (Table 1, entries 11 and 13), the *cis*−*cis* isomers (**11b** and **13b**) were found to be the predominant products after oxidation with a small amount of the other three isomers. For entry 12, a mixture of four isomers was obtained after oxidation with a similar amount of isomers **12a** and **12b**. Thus, substitution of an F at the 5-position of the oxindole ring or removal of a methyl group from the amide nitrogen seemed to favor isomer **b**. These data show that for these compounds, isomerization occurs in CH_3CN and H_2O or in MeOH.

To investigate the isomerization in more detail, we obtained four individual isomers **5a**−**5d** (entry 5) to high purity. Isomer **5a**, **5c** or **5d** each was gradually converted into a mixture of four isomers over a period of up to four days in CH_3CN-H_2O (Figure 2). Isomer **5b**, on the other hand, was quite stable in CH_3CN-H2O, only 4% being converted into a mixture of three other isomers after 12 days.

To determine the absolute stereochemistry of isomer **b**, we obtained the crystal structure of **13b**, which revealed the stereochemistry of three hydrophobic groups in a *cis*−*cis* substitution pattern (*R*-*R*-*S* configuration) on the pyrrolidine ring (Figure 3). The crystal structure of an intermediate after the ring-opening (**14**), however, showed that the substitution pattern of the three hydrophobic groups on the pyrrolidine ring was *trans*−*cis* (*R*-*S*-*R* configuration, Figure 3). Hence, these data indicate that initial product after oxidative removal of the chiral auxiliary has a *trans*−*cis* configuration on the pyrrolidine ring, and upon cleavage of the chiral auxiliary, the isomerization occurs when the final products are exposed to H_2O and MeCN prior to the workup.

On the basis of the X-ray crystallographic data from **13b** and **14**, we propose the reaction mechanism shown in Scheme 2 for the observed isomerization. The *trans*−*cis* isomers **1a**−**13a** (Table 1) are the initial products from CAN oxidation. In aqueous solution, the *trans*−*cis* isomers **1a**−**13a** undergo a

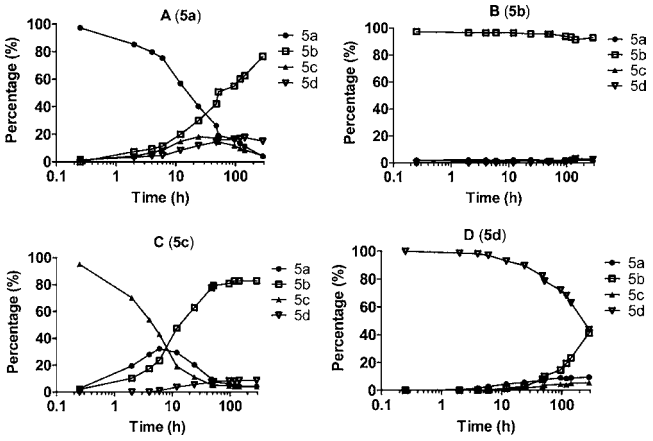

Figure 2. Interconversion of **5a**−**5d** in MeCN−H_2O. Panels A to D show isomerization of compounds **5a**−**5d**. The proportion of compounds is on the *y* axis and reaction time is on the *x* axis. Conditions: Trifluoroacetate salts (0.1 mg) of the amine were placed in 0.25 mL of 50% aqueous MeCN. Purity was analyzed at the indicated time points by analytical reverse phase HPLC.

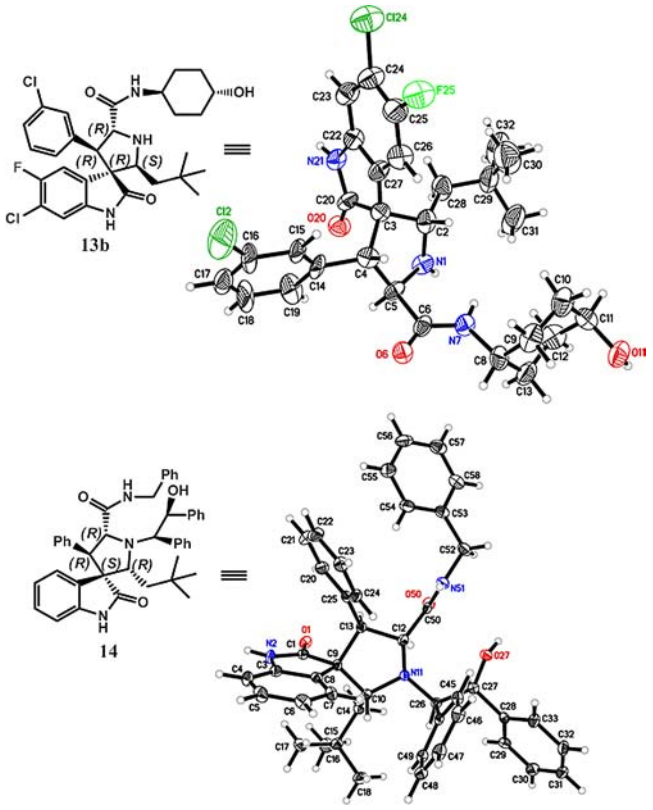

Figure 3. Absolute stereochemistry from X-ray crystallography.

reversible retro-Mannich reaction affording the respective ring-opened transition state (**a**-**TS**) in which the pyrrolidine ring has been opened. Recyclization of **a**-**TS** affords four stereoisomers.[9] We did not attempt to determine the crystal structures of stereoisomers **c** and **d** because very limited amounts of the compounds could be obtained, due to their facile conversion to other isomers. Stereochemistry of isomers **c** and **d** were assigned based on the stability profiles of **5c** and **5d** in Figure 2 and the stereochemistry for isomers **a** and **b**.

We next investigated binding kinetics of isomers **5a**−**5d** to MDM2 in the binding assay medium using our fluorescence-

dx.doi.org/10.1021/ja3125417 | J. Am. Chem. Soc. 2013, 135, 7223−7234

Scheme 2. Proposed Isomerization Mechanism of Spirooxindole-containing Compounds 1a−13a

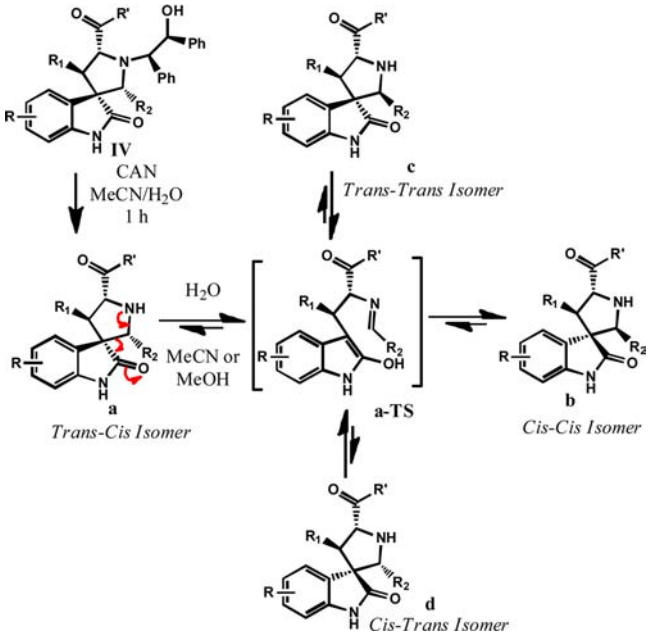

polarization (FP) assay (Figure 4). DMSO stock solutions of **5a**−**5d** were freshly prepared from lyophilized powder of **5a**−**5d** right before the experiments. Then, aqueous incubation solutions of **5a**−**5d** were prepared by diluting the fresh DMSO stock solutions in FP binding assay buffer and final DMSO concentration was 5%. These incubation solutions, in which isomerization of **5a**−**5d** was taking place, were stored at room temperature for the whole time range of experiments. Aliquots of the incubation solutions of **5a**−**5d** were tested at different time points to determine MDM2 binding affinities. Since isomerization of **5a**−**5d** is sensitive to the incubation time, total time used for binding assay plate preparation and incubation was precisely controlled so that assay plates were read exactly 10 min after aliquots were pipetted from the incubation solution.

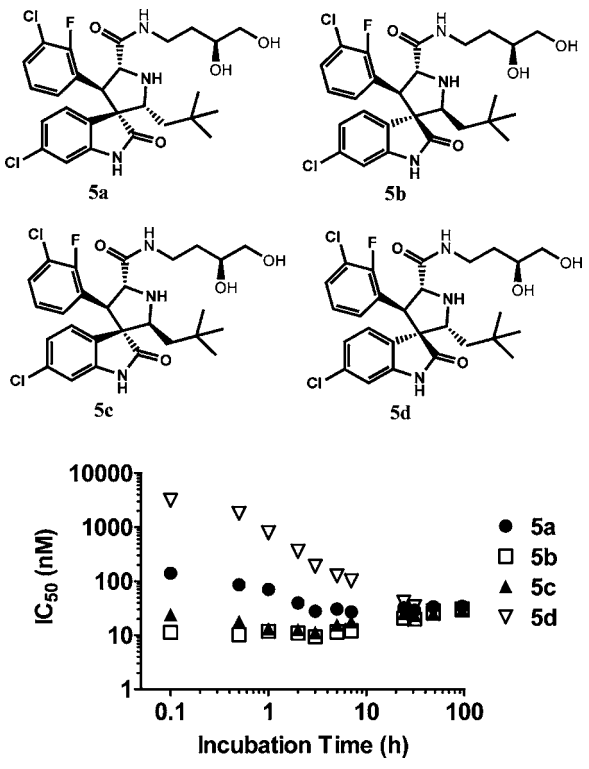

Figure 4. Binding kinetics of **5a**, **5b**, **5c** and **5d**. The IC_{50} of MDM2 binding affinity is on the *y* axis and incubation time is on the *x* axis. See Experimental section for binding assay conditions.

In the first time-point, isomer **5b** has the highest binding affinity, followed by **5c**, **5a**, and **5d** (Figure 4). The stereochemistry has a significant effect on their binding affinity to MDM2; isomer **5b** is >300-times more potent than isomer **5d** and is 18-times more potent than **5a**. However, after 100 h, the binding affinities for these four isomers converged (Figure 4).

To understand the binding kinetics of **5a**−**5d**, we investigated the isomerization kinetics of **5a**−**5d** in binding assay medium by direct HPLC analysis of a solution of the individual compound in binding medium at indicated time points (Figure 5). At the 100 h time-point, there was a similar distribution for each individual isomer, regardless which isomer was used at the beginning, and isomer **5b** and **5a** accounted for approximately 50% and 40%, respectively. Isomer **5b** has a slow isomerization kinetic and was the most stable, followed by isomer **5d**, **5a**, and **5c**. Isomer **5c** had very fast isomerization kinetics and approximately 20% of it was already isomerized into **5b** within 30 min. Hence, the high binding affinity for isomer **5c** in the beginning (Figure 4) should be interpreted with caution since there was a significant amount of **5d** in the binding assay medium. Therefore, the binding kinetics of **5a**−**5d** (Figure 4) is consistent with the observed isomerization kinetics (Figure 5).

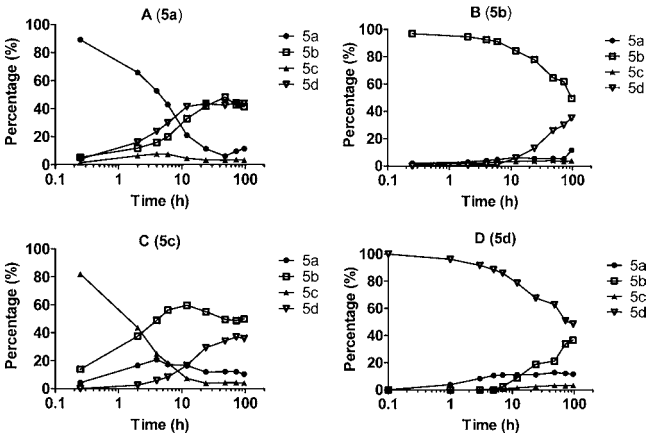

Figure 5. Isomerization of **5a**−**5d** in binding assay medium. Panels A to D correspond to isomerization studies of isomers **5a**−**5d**. The proportion of compounds is on the *y* axis and reaction time is on the *x* axis. Conditions: the individual sample **5a**, **5b**, **5c** or **5b** (0.1 mg) was dissolved in binding medium (0.25 mL) and the samples were incubated at room temperature. The solution of corresponding isomer in binding medium was directly analyzed in analytical reverse phase HPLC at the indicated time points.

We also investigated the isomerization kinetics for **1a**, **1b**, **6a**, **6b**, **12a**, and **12b** in the binding assay medium. Our data showed that in general, isomers **a** isomerized relatively fast, whereas isomers **b** were fairly stable (SI). For instance, after 12 days in the medium, 93.9% of **1b** remained when started with

dx.doi.org/10.1021/ja3125417 | J. Am. Chem. Soc. 2013, 135, 7223−7234

Table 2. Binding Affinity of Selected Spirooxindole Inhibitors to MDM2 Protein

entry	compound[a,b]	IC_{50}[c] (nM)	K_i[d] (nM)	compound[a,b]	IC_{50}[c] (nM)	K_i[d] (nM)
1	**1a**	10700 ± 1300	1500 ± 180	**1b**	126 ± 13	16.1 ± 1.7
2	**2a**	565 ± 57	76.2 ± 7.7	**2b**	30.9 ± 2.9	3.1 ± 0.3
3	**3a**[b]	2285 ± 183	311 ± 24	**3b**	137 ± 11	17.6 ± 1.0
4	**4a**	387 ± 39	51.8 ± 4.2	**4b**	25.9 ± 1.5	2.4 ± 0.2
5	**5a**	141 ± 11	18.1 ± 1.0	**5b**	11.3 ± 1.2	1.0
6	**6a**[b]	410 ± 39	54.9 ± 4.2	**6b**	24.6 ± 7.0	2.2 ± 0.5
7	**7a**	19500 ± 4000	2700 ± 500	**7b**	721 ± 79	97.5 ± 10.7
8	**8a**	498 ± 44	67.0 ± 5.9	**8b**	55.1 ± 5.2	6.4 ± 0.6
9	**9a**	n.d.[e]		**9b**	22.5 ± 2.2	1.9 ± 0.2
10	**10a**	n.d.[e]		**10b**	835 ± 121	113 ± 16
11	**11a**	n.d.[e]		**11b**	112 ± 12	14.2 ± 1.1
12	**12a**[b]	180 ± 24	23.5 ± 2.1	**12b**	104 ± 16	13.1 ± 1.0
13	**13a**	n.d.[e]		**13b**	66.8 ± 7.4	8.0 ± 1.0
14	**1d**	181000 ± 31000	25000 ± 18000			
15	**5c**	24.1 ± 2.3	2.2 ± 0.2	**5d**	3100 ± 460	430 ± 62

[a]Purity was >95% unless otherwise stated. [b]Purity of **4a** was 94%; of **6a**, 93.5% and of **12a**, 82%. [c]See Experimental section for binding assay procedures. [d]Calculation of K_i based on IC_{50}.[10] [e]n.d. not determined.

1b but 53% of **1a** converted into **1b** and only 17.6% of **1a** remained when started with **1a**.

We purified a sufficient amount of *cis*−*cis* isomers **1b**−**13b** and *trans*−*cis* isomer **1a**−**8a** and **12a** and determined their binding affinities to MDM2 (Table 2). Upon the basis of the isomerization kinetics observed for **5a**/**5b**, **1a**/**1b**, **6a**/**6b** and **12a**/**12b**, there was minimal isomerization for these isomers in the binding assay medium in the initial 20 min. Therefore, the incubation time in all binding experiments was controlled precisely at 15 min, resulting in less than 20 min experimental time in total, including plate preparation and incubation, to minimize the influence of the isomerization on MDM2 binding affinity. Our binding data showed that in general, the *cis*−*cis* isomers **b** have better binding affinities to MDM2 than the corresponding *trans*−*cis* isomers **a**. For example, **4b** and **5b** are >15-times more potent than their respective isomer **4a** and **5a**. Interestingly, **12a** and **12b** have very similar binding affinities.

Our binding data also provided initial structure−activity relationship for isomers **b**. Substitution of F at the 2-position of the phenyl ring of **1b** and **2b** has no effect on the MDM2 binding affinity (compare **1b** versus **3b** and **2b** versus **4b**). However, substitution of F at the 5-position of the oxindole ring of **1b** and **2b** was detrimental to binding, as shown by the binding affinity difference between **1b** and **10b**, and between **2b** and **11b**. Removal of one methyl from the amide improves the binding affinity of **1b**, **3b**, **4b** and **10b** (compare **1b** versus **2b**, **3b** versus **4b**, **4b** versus **9b** and **10b** versus **11b**). Changing the amide of **9b** to either an ester (**7b**) or an acid (**8b**) decreased the binding affinity to MDM2.

We investigated the cell growth inhibitory activity of isomers **5a** and **5b** in the SJSA-1 osteosarcoma cell line, which has an amplified MDM2 gene and has been extensively used for evaluation of MDM2 inhibitors (Table 3).[6]

Surprisingly, our data showed that despite the difference in their binding affinities to MDM2, there is no significant difference in their activity against cellular growth of the SJSA-1 cell line. To investigate this discrepancy between binding affinities and cellular activities of these two compounds, we monitored the isomerization of **5a** and **5b** in cell culture medium by HPLC analysis of MeCN extracts of cell growth medium containing **5a** or **5b** at indicated time points (Figure 6). Both **5a** and **5b** were found to isomerize in cell growth

Table 3. Cell Growth Inhibitory Activity of 5a and 5b with Different Treatment Time

time	IC_{50} of **5a** (μM)	IC_{50} of **5b** (μM)
Day 1	30.32 ± 6.23	18.06 ± 2.40
Day 2	0.95 ± 0.16	0.63 ± 0.04
Day 3	0.18 ± 0.02	0.18 ± 0.01
Day 4	0.15 ± 0.03	0.14 ± 0.05

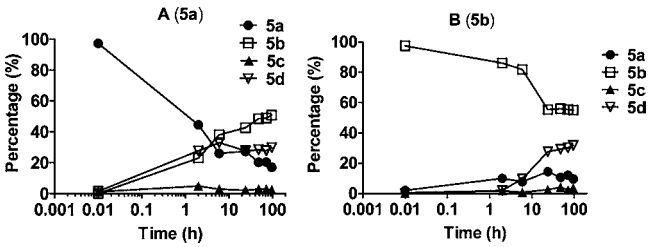

Figure 6. Isomerization studies of **5a** and **5b** in cell culture medium. Panels A and B depict the isomerization studies of compounds **5a** and **5b**, respectively. The proportion of compounds is on the *y* axis and reaction time is on the *x* axis. See SI for conditions of the isomerization study in cell growth inhibition assay medium.

medium (Figure 6, panels 1 and 2). Starting from either **5a** or **5b**, the distributions of four isomers were very similar after incubation for one day in the cell culture medium. After incubation for 2 days, the most potent stereoisomer **5b** in the binding assay accounts for approximately 50% of all 4 isomers, either starting from **5a** or from **5b**. Hence, the relatively rapid isomerization of both **5a** and **5b** in the cell culture medium explains why these two isomers show similar activity in the cell growth inhibitory assay.

We next investigated the *in vivo* activity of **5a** and **5b** in a pharmacodynamic (PD) experiment using SJSA-1 osteosarcoma tumor xenografts in severe combined immunodeficient (SCID) mice. SCID mice bearing SJSA-1 tumors were treated with a single dose of **5a** or **5b** at 200 mg/kg via oral gavage and the tumor tissues were harvested at indicated time points for Western blotting analysis of p53 activation. Western blotting showed that both **5a** and **5b** effectively activated p53 in tumor tissue in a time-dependent manner, as shown by the

dx.doi.org/10.1021/ja3125417 | J. Am. Chem. Soc. 2013, 135, 7223−7234

accumulation of p53 protein itself, and MDM2 and p21 proteins, two p53 targeted gene products (Figure 7).

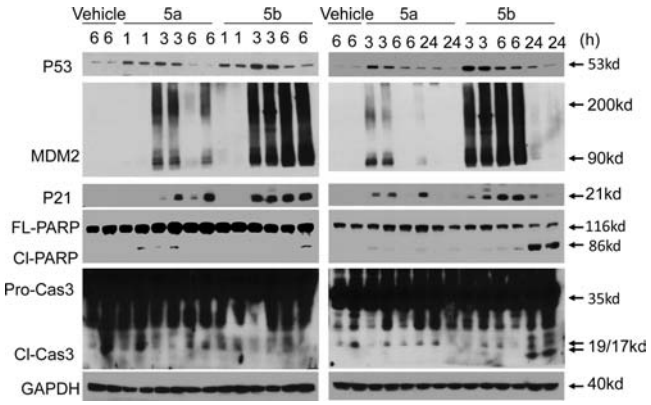

Figure 7. Western blot analysis of p53 activation induced by **5a** and **5b** in SJSA-1 osteosarcoma tumor tissue with a single, oral dose of either compound at 200 mg/kg. FL-PARP, full-length PAPR; Cl-PARP, cleaved PARP; Pro-Cas3, pro-caspase-3; Cl-Cas3, cleaved caspase-3.

Isomer **5b** was clearly more potent than **5a** in activating p53 in tumor tissues. At 24 h, **5b** resulted in stronger apoptosis induction than **5a** based upon cleavage of poly(ADP-ribose) polymerase (PARP) and activation of caspase-3, two biochemical markers of apoptosis. These PD data in tumor-bearing mice demonstrate that isomer **5b** is more potent than isomer **5a** *in vivo* in activation of p53 and induction of apoptosis, in contrast to the cell growth data observed in these two isomers (Table 3).

To further understand the clear difference between isomers **5a** and **5b** in the *in vivo* PD experiment in SJSA-1 tumor tissue, we investigated the isomerization of **5a** and **5b** *in vivo* in both plasma and tumor tissue in SCID mice bearing SJSA-1 tumors. SCID mice were orally administered with a single, oral dose of **5a** or **5b** at 100 mg/kg, and samples of plasma and tumor tissue were collected at 1, 6, and 24 h and analyzed using the LC-MS/MS method. The data are summarized in Table 4.

In plasma, the concentration of **5b** in mice dosed with **5b** was 7-fold higher than that in mice dosed with **5a** at 1 h and was 12-fold at 6 h. In tumor tissue, the concentration of **5b** in mice dosed with **5b** was 11-fold higher than that in mice dosed with **5a** at 1 h, and was 16-fold at 6 h. Hence, the much stronger induction of p53 activation and of PARP cleavage by **5b** than **5a** in SJSA-1 tumor tissue (Figure 7) is consistent with the data that much higher concentrations of **5b** were achieved when dosed with **5b** than dosed with **5a** in tumor tissue, and **5b** is 18-times more potent than **5a** in terms of binding to MDM2.

Table 4. Concentration of 5a and 5b in Plasma and Tumor Tissue in SCID Mice Bearing SJSA-1 Tumors when Dosed with Either 5a or 5b

dosing	isomer	1 h	6 h	24 h
		Plasma concentration (ng/mL)[a]		
5b	**5b**	16800 ± 1931	2577 ± 815	5.9 ± 0.8
	5a	3343 ± 1385	47 ± 20	BLQ[b]
5a	**5b**	2380 ± 448	210 ± 141	BLQ
	5a	617 ± 97	75 ± 24	BLQ
		Tumor concentration(ng/g)[a]		
5b	**5b**	19133 ± 3775	1963 ± 683	BLQ
	5a	1122 ± 297	65 ± 24	BLQ
5a	**5b**	1797 ± 527	120 ± 84	BLQ
	5a	2973 ± 1036	27 ± 18	BLQ

[a]Three mice per time point. [b]BLQ: below the lower limit of quantification.

To further analyze isomerization of compound **5** *in vivo*, we determined the ratio of four isomers (**5a**–**5d**) when dosed with either **5a** or **5b** based upon the HPLC spectra from analysis of the extracts of plasma and tumor tissue homogenate (Figure 8).

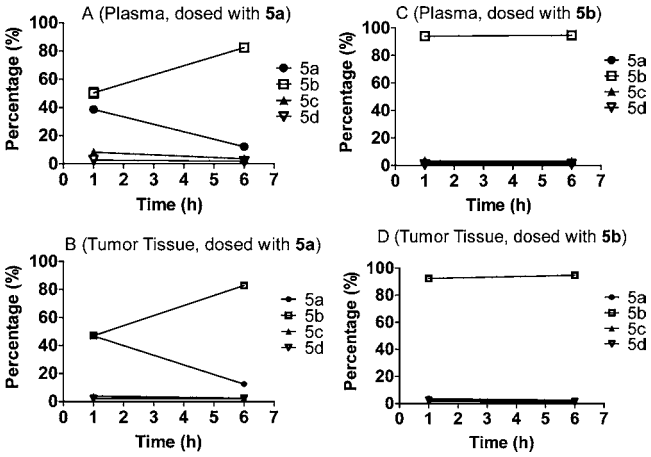

Figure 8. Isomerization of **5a** and **5b** in tumor tissue or plasma. Panels A and B depict the isomerization of **5a** and panels C and D depict the isomerization of **5b** in plasma and tumor tissue accordingly. The proportion of compounds is on the *y* axis and the time when samples were harvested is on the *x* axis. Bars indicate the standard error.

Our data showed that when dosed with **5b**, **5b** remained the dominant isomer at 1 and 6 h time-points and there was only a small percentage of the other three isomers (<10% when combined). In contrast, when dosed with **5a**, there was rapid isomerization and isomer **5b** became the dominant form at the 6 h time-point. These data show that **5b** isomerizes slowly *in vivo* whereas **5a** isomerizes very fast.

We determined the antitumor activity of **5a** and **5b** in the SJSA-1 xenograft model. SCID mice bearing established SJSA-1 tumors were treated with **5a** at 200 mg/kg or **5b** at 100 mg/kg and 200 mg/kg daily *via* oral gavage for 14 days (Figure 9). Isomer **5a** at 200 mg/kg daily dosing inhibited tumor growth by 41% as compared to vehicle control ($p < 0.0001$) at the end of the treatment (day 26). In comparison, **5b** at 100 mg/kg inhibited tumor growth by 67% ($p < 0.0001$) but shrank tumors at 200 mg/kg by an average of 91% at the end of treatment (day 26, see SI). There was no significant weight loss (SI) or

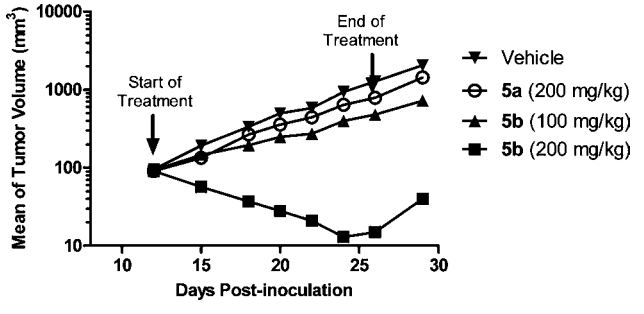

Figure 9. Antitumor activity of **5a** and **5b** in the SJSA-1 osteosarcoma tumor xenograft model.

dx.doi.org/10.1021/ja3125417 | J. Am. Chem. Soc. 2013, 135, 7223–7234

other signs of toxicity for either compound. The efficacy data show that isomer **5b** has much better *in vivo* antitumor activity than isomer **5a**, consistent with the much stronger p53 activation and apoptosis induction by **5b** than by **5a** in tumor tissues (Figure 7).

Although **5b** had a strong antitumor activity and shrank tumors by 91% in the SJSA-1 xenograft model, it failed to achieve complete tumor regression. We hypothesized that the failure of complete tumor regression by **5b** may be due to its less than ideal pharmacokinetic (PK) properties. To this end, we have performed extensive modifications to spirooxindol-containing compounds to further improve their *in vivo* PK profile, which ultimately led to identification of compound **15b** (**MI-888**) (Figure 10).[12] Compound **15b** binds to MDM2 with

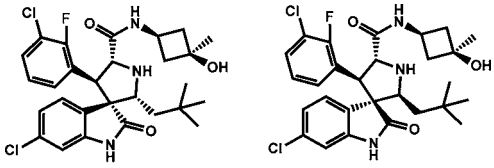

Figure 10. Structures and MDM2 binding affinity of **15a** and **15b**.

a K_i value of 0.44 nM. In comparison, the corresponding *cis*–*trans* isomer **15a** has a K_i value of 4.5 nM in binding to MDM2, being 10-times less potent than **15b**.

To test the therapeutic potential and the potential difference in their antitumor activity between **15a** and **15b**, both compounds were tested in the SJSA-1 tumor xenograft model. In this experiment, SCID mice bearing established SJSA-1 tumors were treated with **15a** at 100 mg/kg or **15b** at 100 mg/kg via oral gavage for 14 days (Figure 11).

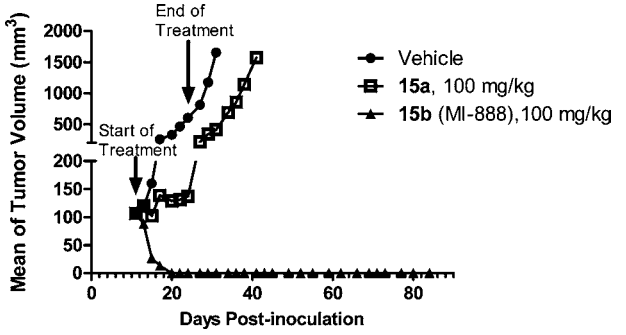

Figure 11. Antitumor activity of **15a** and **15b** in the SJSA-1 osteosarcoma tumor xenograft model.

In contrast to **5b**, and other previously reported potent MDM2 inhibitors, such as MI-219, Nutlin-3a and AM-8553,[6b,13] **15b** was capable of achieving rapid and complete tumor regression. After treatments with **15b** for 10 days at 100 mg/kg, all tumors of the treated mice completely regressed. Importantly, the complete regression was long-lasting; all mice treated with **15b** remained completely tumor free for an additional 64 days. In comparison, while **15a** at 100 mg/kg daily dosing inhibited tumor growth by 78% as compared to vehicle control ($p < 0.0001$) at the end of the treatment (day 24), it failed to achieve tumor regression. There was no significant weight loss or other signs of toxicity for either compound (SI). The efficacy data thus clearly demonstrate that isomer **15b** is much more efficacious than isomer **15a**.

CONCLUSIONS

In the present study, we have performed detailed investigations on the reversible ring-opening-recyclization reaction of selected spirooxindole-containing MDM2 inhibitors. This reaction afforded four diastereoisomers from one single stereoisomer. The stable isomers (isomers **b**) for these compounds have a *cis*–*cis* configuration and bind to MDM2 with better affinities than the other three isomers. Importantly, our investigation has led to the identification of a set of highly potent MDM2 inhibitors with a low nanomolar binding affinity. In particular, compound **15b** (**MI-888**) has a K_i value of 0.44 nM to MDM2 and is capable of achieving complete and long-lasting tumor regression in an animal model of human cancer. Our data clearly suggest that **MI-888** is a highly promising MDM2 inhibitor and warrants extensive preclinical investigation as a potential clinical development candidate.

EXPERIMENTAL SECTION

1. Chemistry. All reactions were conducted in round-bottomed flasks with a Teflon-coated magnet stirring bar. Experiments involving moisture and/or air sensitive components were performed under an N_2 atmosphere. Commercial reagents and anhydrous solvents were used without further purification. Crude reaction products were purified by flash column chromatography on silica gel. Further purification was performed on a semipreparative HPLC (Waters Delta 600) with SunFire C18 reverse phase column (19 mm × 150 mm). The mobile phase was a gradient flow of solvent A (water, 0.1% of TFA) and solvent B (CH_3CN, 0.1% of TFA or MeOH, 0.1% of TFA) at a flow rate of 10 mL/min. Proton nuclear magnetic resonance (^{1}H NMR) and carbon nuclear magnetic resonance (^{13}C NMR) spectroscopy were performed on a Bruker Advance 300 NMR spectrometer. Low resolution ESI mass spectra analyses were determined on a Thermo-Scientific LCQ Fleet mass spectrometer. The analytical reverse phase HPLC (rp-HPLC) model was Waters 2795 Separation (UV detection at 230 and 254 nm wavelengths). All final compounds were purified to ≥95% purity as determined by analytical HPLC analysis using reverse phase column (SunFire, C18–5 μm, 4.6 × 150 mm) unless otherwise stated.

The procedures for synthesis of compounds **1a**–**6a**, **12a**, and **15a** were adapted from our previously reported methods[6d,7] shown in Scheme 1 with some modifications.[6a] The *trans*–*cis* isomers **1a**–**6a** and **15a** were obtained as major products after ceric ammonium nitrate (CAN) oxidative cleavage of chiral auxiliary. The *trans*–*cis* isomers **9a**, **11a**, and **13a** were minor isomers after CAN oxidation and efforts made to obtain **9a**–**13a** in high purity proved futile.

Detailed procedures for the synthesis of **7a** and **8a** via different synthetic routes are in the Supporting Information (SI).

*(2′R,3S,4′R,5′R)-6-Chloro-4′-(3-chlorophenyl)-N,N-dimethyl-2′-neopentyl-2-oxospiro[indoline-3,3′-pyrrolidine]-5′-carboxamide (**1a**, TFA salt).* ^{1}H NMR (300 MHz, CD_3OD): 7.40–7.32 (m, 4H), 6.87 (s, 1H), 6.76 (d, J = 8.22 Hz, 1H), 6.55 (d, J = 8.17 Hz, 1H), 5.47 (d, J = 7.88 Hz, 1H), 4.28 (d, J = 6.38 Hz, 1H), 4.17 (d, J = 7.88 Hz, 1H), 2.97 (s, 3H), 2.78 (s, 3H), 2.05 (dd, J = 15.31, 7.63, Hz, 1H), 1.16 (d, J = 15.31 Hz, 1H), 0.84 (s, 9H). ^{13}C (75 MHz, CD_3OD): 180.46, 167.42, 145.49, 139.42, 136.92, 136.38, 131.97, 130.50, 130.23, 128.37, 128.30, 124.57, 123.26, 112.09, 63.35, 63.27, 62.84, 55.37, 42.47, 38.03, 36.96, 30.99, 29.59. ESI-MS calculated for $C_{25}H_{30}{}^{35}Cl_2N_3O_2$ $[M + H]^+$ = 474.17, Found: 474.50. $[\alpha]_D{}^{25}$ = −40.4° (c = 0.0113, MeCN)

*(2′R,3S,4′R,5′R)-6-Chloro-4′-(3-chlorophenyl)-N-methyl-2′-neopentyl-2-oxospiro[indoline-3,3′-pyrrolidine]-5′-carboxamide (**2a**, TFA salt).* ^{1}H NMR (300 MHz, CD_3OD): 7.28–7.16 (m, 3H), 7.16–7.06 (m, 1H), 6.92–6.82 (m, 2H), 6.80–6.76 (m, 1H), 4.92 (d, J = 10.23, 4.20–4.10 (m, 2H), 2.73 (s, 3H), 1.99 (s, J = 15.32, 6.75 Hz, 1H), 1.47 (dd, J = 15.54, 3.49 Hz, 1H), 0.80 (s, 9H). ^{13}C (75 MHz,

dx.doi.org/10.1021/ja3125417 | J. Am. Chem. Soc. 2013, 135, 7223–7234

CD_3OD): 180.04, 167.26, 144.79, 137.00, 136.58, 135.84, 131.40, 129.99, 129.84, 128.18, 128.11, 126.71, 123.42, 111.88, 64.23, 64.23, 62.35, 57.08, 42.71, 30.95, 29.58, 27.00. ESI-MS calculated for $C_{24}H_{28}{}^{35}Cl_2N_3O_2$ $[M + H]^+$ = 460.16, Found: 460.52

*(2′R,3S,4′S,5′R)-6-Chloro-4′-(3-chloro-2-fluorophenyl)-N,N-dimethyl-2′-neopentyl-2-oxospiro[indoline-3,3′-pyrrolidine]-5′-carboxamide (**3a**, TFA salt).* ^{1}H NMR (300 MHz, CD_3OD): 7.80−7.70 (m, 1H), 7.50−7.40 (m, 1H), 7.32−7.22 (m, 1H), 6.92−6.88 (m, 1H), 6.74 (dd, J = 8.15, 1.75 Hz, 1H), 6.48 (d, J = 8.11 Hz, 1H), 5.58 (d, J = 7.94 Hz, 1H), 4.38 (d, J = 7.94 Hz, 1H), 4.26 (d, J = 7.55 Hz, 1H), 2.99 (s, 3H), 2.84 (s, 3H), 2.06 (dd, J = 15.42, 7.72 Hz, 1H), 1.13 (d, J = 15.37 Hz, 1H), 0.89 (s, 9H). ^{13}C (75 MHz, CD_3OD): 180.07, 166.93, 157.51 (d, J_{C-F} = 243.98 Hz), 145.59, 137.11, 132.54, 128.77, 127.66, 126.74 (d, J_{C-F} = 4.55 Hz), 125.89 (d, J_{C-F} =13.40 Hz), 123.68, 122.85 (d, J_{C-F} = 10.19 Hz), 123.10 (d, J_{C-F} = 18.37 Hz), 112.07, 63.03, 62.05, 61.76, 42.09, 37.70, 36.89, 30.77, 29.34. ESI-MS calculated for $C_{25}H_{29}{}^{35}Cl_2FN_3O_2$ $[M + H]^+$ = 492.16, Found: 492.44

*(2′R,3S,4′S,5′R)-6-Chloro-4′-(3-chloro-2-fluorophenyl)-N-methyl-2′-neopentyl-2-oxospiro[indoline-3,3′-pyrrolidine]-5′-carboxamide (**4a**, TFA salt, 94% purity).* ^{1}H NMR (300 MHz, CD_3OD): 7.66−7.54 (m, 1H), 7.38−7.28 (m, 1H), 7.22−7.10 (m, 1H), 6.87 (s, 1H), 6.82−6.72 (m, 2H), 5.21 (d, J = 10.00 Hz, 1H), 4.50 (d, J = 9.93 Hz, 1H), 4.30−4.24 (m, 1H), 2.75 (s, 3H), 2.07 (dd, J = 15.35, 7.35 Hz, 1H), 1.8 (d, J = 14.57 Hz, 1H), 0.80 (s, 9H). ^{13}C (75 MHz, CD_3OD): 180.31, 167.24, 157.81 (d, J_{C-F} = 247.78 Hz), 145.44, 136.94, 132.11, 128.66, 127.94, 126.47 (d, J_{C-F} = 4.45 Hz), 125.29, 125.01 (d, J_{C-F} = 13.96 Hz), 123.37, 122.64 (d, J_{C-F} = 18.03 Hz), 122.04, 64.35, 63.69, 61.74, 49.51, 42.34, 30.92, 29.55, 27.10. ESI-MS calculated for $C_{24}H_{27}{}^{35}Cl_2FN_3O_2$ $[M + H]^+$ = 478.15, Found: 478.92

*(2′R,3S,4′S,5′R)-6-Chloro-4′-(3-chloro-2-fluorophenyl)-N-((S)-3,4-dihydroxybutyl)-2′-neopentyl-2-oxospiro[indoline-3,3′-pyrrolidine]-5′-carboxamide (**5a**, TFA salt).* ^{1}H NMR (300 MHz, CD_3OD): 7.63−7.53 (m, 1H), 7.40−7.30 (m, 1H), 7.23−7.13 (m, 1H), 6.87 (d, J = 1.36 Hz, 1H), 6.86−6.74 (m, 2H), 5.19 (d, J = 10.22 Hz, 1H), 4.49 (d, J = 10.22 Hz,1H), 4.25 (dd, J = 7.35, 2.71 Hz, 1H), 3.56−3.43 (m, 1H), 3.42−3.30 (m, 4H), 2.07 (dd, J = 15.43, 7.44 Hz,1 H), 1.72−1.58 (m, 1H), 1.56−1.40 (m, 1H), 1.30 (dd, J = 15.43, 2.62 Hz, 1H), 0.80 (s, 9H). ^{13}C (75 MHz, CD_3OD): 180.26, 166.78, 157.81 (d, J_{C-F} = 247.93 Hz), 145.43, 136.90, 132.16, 128.82, 127.96, 126.48 (d, J_{C-F} = 4.49 Hz), 125.43, 124.94 (d, J_{C-F} = 14.00 Hz), 123.37, 122.63 (d, J_{C-F} = 18.23 Hz), 112.00, 71.01, 67.25, 64.38, 63.80, 61.69, 50.06, 42.36, 38.30, 33.80, 30.94, 29.55. ESI-MS calculated for $C_{27}H_{33}{}^{35}Cl_2FN_3O_4$ $[M + H]^+$ = 552.18, Found: 552.92; $[\alpha]_D{}^{25}$ = −40.1° (c = 0.0106, MeOH)

*(2′R,3S,4′S,5′R)-6-Chloro-4′-(3-chloro-2-fluorophenyl)-N-(2-morpholinoethyl)-2′-neopentyl-2-oxospiro[indoline-3,3′-pyrrolidine]-5′-carboxamide (**6a**, TFA salt, 93.5% purity).* ^{1}H NMR (300 MHz, CD_3OD): 7.59 (t, J = 6.93 Hz, 1H), 7.41 (td, J = 7.55, 0.97 Hz, 1H), 7.22 (t, J = 7.90 Hz, 1H), 6.90 (d, J = 1.79 Hz, 1H), 6.77 (dd, J = 8.14, 1.79 Hz, 1H), 6.48 (d, J = 8.15 Hz, 1H), 5.21 (d, J = 8.22 Hz, 1H), 4.50 (d, J = 8.19 Hz, 1H), 4.17 (dd, J = 7.63, 2.23 Hz, 1H), 4.10−3.80 (m, 4H), 3.75−3.45 (m, 4H), 3.40−3.00 (m, 4H), 2.08−1.96 (m, 1H), 1.19 (dd, J = 15.32, 2.23 Hz, 1H), 0.81 (s, 9H). ^{13}C (75 MHz, CD_3OD): 180.28, 168.91, 157.75 (d, J_{C-F} = 248.38 Hz), 145.50, 137.13, 132.29, 128.63, 127.67, 126.63 (d, J_{C-F} = 4.50 Hz), 125.74 (d, J_{C-F} = 13.69 Hz), 124.72, 123.44, 122.83 (d, J_{C-F} = 18.25 Hz), 112.20, 65.16, 64.25, 63.84, 62.22, 58.01, 53.84, 50.05, 42.39, 35.72, 30.95, 29.52. ESI-MS calculated for $C_{29}H_{36}{}^{35}Cl_2FN_4O_3$ $[M + H]^+$ = 577.21, Found: 577.48. $[\alpha]_D{}^{25}$ = −43.3° (c = 0.0139, MeCN).

*(2′R,3S,4′S,5′R)-Ethyl 6-Chloro-4′-(3-chloro-2-fluorophenyl)-2′-neopentyl-2-oxospiro[indoline-3,3′-pyrrolidine]-5′-carboxylate (**7a**, TFA salt).* ^{1}H NMR (300 MHz, CD_3OD): 7.50−7.40 (m, 2H), 7.28−7.18 (m, 1H), 6.91 (d, J = 1.81 Hz, 1H), 6.78(dd, J = 8.13, 1.87 Hz, 1H), 6.46 (d, J = 8.14 Hz, 1H), 5.30 (d, J = 8.52 Hz, 1H), 4.43 (d, J = 8.52 Hz, 1H), 4.40−4.20 (m, 2H), 4.08 (dd, J = 7.47, 2.43 Hz, 1H), 2.00 (dd, J = 15.32, 7.53 Hz, 1H), 1.22 (t, J = 7.12 Hz, 3H), 1.19 (dd, J = 15.32, 2.55 Hz, 1H), 0.81 (s, 9H). ^{13}C (75 MHz, CD_3Cl, note free amine): 181.33, 171.91, 156.54 (d, J_{C-F} = 248.02 Hz), 142.85, 134.15, 129.91, 128.37 (d, J_{C-F} = 14.61 Hz), 127.19 (d, J_{C-F} = 3.19 Hz), 125.94, 124.94, 124.63 (d, J_{C-F} = 4.50 Hz), 122.10, 121.69 (d, J_{C-F} = 18.50 Hz), 110.72, 67.16, 65.70, 63.19, 61.74, 51.17, 43.45, 30.33, 29.97, 14.32. ESI-MS calculated for $C_{25}H_{28}{}^{35}Cl_2FN_2O_3$ $[M + H]^+$ = 493.15, Found: 493.44

*(2′R,3S,4′S,5′R)-6-Chloro-4′-(3-chloro-2-fluorophenyl)-2′-neopentyl-2-oxospiro[indoline-3,3′-pyrrolidine]-5′-carboxylic acid (**8a**, TFA salt).* ^{1}H NMR (300 MHz, CD_3OD): 7.56−7.46 (m, 1H), 7.46−7.36 (m, 1H), 7.26−7.18 (m, 1H), 6.91 (d, J = 1.61 Hz, 1H), 6.76 (dd, J = 8.10, 1.50 Hz, 1H), 6.47 (d, J = 8.14 Hz, 1H), 5.29 (d, J = 8.67 Hz, 1H), 4.43 (d, J = 8.67 Hz, 1H), 4.11 (d, J = 7.47, 2.13 Hz, 1H), 2.02 (dd, J = 15.36, 7.50 Hz, 1H), 1.16 (dd, J = 15.36, 2.24 Hz, 1H), 0.81 (s, 9H). ESI-MS calculated for $C_{23}H_{24}{}^{35}Cl_2FN_2O_3$ $[M + H]^+$ = 465.11, Found: 465.42;

*(2′R,3S,4′R,5′R)-6-Chloro-4′-(3-chlorophenyl)-N-((S)-3,4-dihydroxybutyl)-5-fluoro-2′-neopentyl-2-oxospiro[indoline-3,3′-pyrrolidine]-5′-carboxamide (**12a**, TFA salt, 82% purity).* ^{1}H NMR (300 MHz, CD_3OD): 7.32−7.22 (m, 3H), 7.18−7.10 (m, 1H), 7.06 (d, J = 8.74 Hz, 1H), 6.88 (d, J = 6.08 Hz, 1H), 4.97 (d, J = 10.79 Hz, 1H), 4.22 (d, J = 10.79 Hz, 1H), 4.26−4.18 (m, 1H), 3.50−3.20 (m, 5H), 2.03 (dd, J = 15.35, 6.56 Hz, 1H), 1.68−1.52 (m, 2H), 1.50−1.40 (m, 1H), 0.84 (s, 9H). ^{13}C (75 MHz, CD_3OD): 179.64, 166.47, 140.40 (d, J_{C-F} = 2.94 Hz), 136.54, 136.06, 131.64, 130.16, 130.02, 128.14, 127.27 (d, J_{C-F} = 40.14 Hz), 123.05 (d, J_{C-F} = 19.44 Hz), 115.94 (d, J_{C-F} = 25.54 Hz), 113.09, 70.91, 67.24, 64.19, 64.10, 62.73, 57.52, 42.66, 38.14, 33.85, 30.99, 29.57. ESI-MS calculated for $C_{27}H_{33}{}^{35}Cl_2FN_3O_4$ $[M + H]^+$ = 552.18, Found: 552.75

*(2′R,3S,4′R,5′R)-6-Chloro-4′-(3-chlorophenyl)-N-((1s,3S)-3-hydroxy-3-methylcyclobutyl)-2′-neopentyl-2-oxospiro[indoline-3,3′-pyrrolidine]-5′-carboxamide (**15a**, TFA salt).* ^{1}H NMR (300 MHz, MeOD-d_4): 7.40−7.50 (m, 1H), 7.40−7.30 (m, 1H), 7.20−7.10 (m, 1H), 6.85 (s, 1H), 6.83−6.75 (m, 2H), 5.11 (d, J = 10.11 Hz, 1H), 4.47 (d, J = 10.09 Hz, 1H), 4.22 (dd, J = 7.32, 2.72 Hz, 1H), 4.00−3.80 (m, 1H), 2.50−2.30 (m, 2H), 2.15−1.95 (m, 2H), 1.95−1.80 (m, 1H), 1.40−1.20 (m, 1H), 1.29 (s, 3H), 0.80 (s, 9H). ^{13}C NMR (75 MHz, MeOD-d_4): 180.0, 165.9, 157.6 (d, J_{C-F} = 248 Hz), 145.3, 136.7, 131.9, 128.6, 127.7, 126.2 (d, J_{C-F} = 4.76 Hz), 125.2, 124.8 (d, J_{C-F} = 13.8 Hz), 123.1, 122.4 (d, J_{C-F} = 18.1 Hz), 111.8, 64.2, 63.5, 61.4, 49.7, 45.5, 45.4, 42.2, 38.4, 30.7, 29.4, 27.4. ESI-MS calculated for $C_{28}H_{33}{}^{35}Cl_2FN_3O_3$ $[M + H]^+$: 548.17, Found: 548.25. $[\alpha]_D{}^{25}$ = −30.6° (c = 0.0154 g/mL in MeOH);

The *cis*−*cis* isomers **1b**−**7b**, **10b**, **12b**, and **15b** were obtained as major products after aging the materials purified by flash column chromatography in appropriate solvents for 3−4 days. In cases of **9b**, **11b**, and **13b**, the *cis*−*cis* isomers were obtained as major products after the CAN oxidation without aging. Generally, the side isomers **c** and **d** were observed in small amounts after oxidation or after aging.

Standard procedure for aging: 30 mg material obtained from CAN oxidation (prepurified by flash column chromatography) was placed in a round bottomed flask with a magnetic stirring bar. MeCN (2.4 mL) was added to dissolve the product. H_2O (2.0 mL) was added to this MeCN solution followed by 0.4 mL $NaHCO_3$ saturated solution to adjust the pH to 8. This solution was allowed to stir at room temperature for 3−4 days. The percentage of isomer **b** and other isomers was determined using analytical HPLC. Further purification was performed by semipreparative or preparative HPLC. Pure MeOH can also be used as aging solvent.

*(2′S,3R,4′R,5′R)-6-Chloro-4′-(3-chlorophenyl)-N,N-dimethyl-2′-neopentyl-2-oxospiro[indoline-3,3′-pyrrolidine]-5′-carboxamide (**1b**, TFA salt).* ^{1}H NMR (300 MHz, CD_3OD): 7.58 (d, J = 8.08 Hz, 1H), 7.32−7.10 (m, 5H), 6.78 (d, J = 1.54 Hz, 1H), 5.69 (d, J = 10.03 Hz, 1H), 4.41 (d, J = 6.93 Hz, 1H), 4.14 (d, J = 10.03 Hz, 1H), 2.96 (s, 3H), 2.76 (s, 3H), 1.90 (dd, J = 15.41, 8.26 Hz, 1H), 1.15 (d, J = 15.41 Hz, 1H), 0.89 (s, 9H). ^{13}C (75 MHz, CD_3OD): 178.04, 168.67, 145.47, 137.24, 135.99, 135.36, 131.69, 130.50, 129.79, 128.44, 126.49, 124.27, 123.84, 112.31, 65.29, 64.52, 60.50, 57.35, 42.59, 38.06, 37.00, 31.03, 29.66. ESI-MS calculated for $C_{25}H_{30}{}^{35}Cl_2N_3O_2$ $[M + H]^+$ = 474.17, Found: 474.68. $[\alpha]_D{}^{25}$ = 32.1° (c = 0.0126, MeCN).

*(2′R,3R,4′R,5′R)-6-Chloro-4′-(3-chlorophenyl)-N,N-dimethyl-2′-neopentyl-2-oxospiro[indoline-3,3′-pyrrolidine]-5′-carboxamide (**1d**, TFA salt).* ^{1}H NMR (300 MHz, CD_3OD): 7.72 (d, J = 8.08 Hz, 1H), 7.28−7.22 (m, 1H), 7.20−7.12 (m, 2H), 7.12−7.08 (m, 1H), 7.04 (d, J = 7.65 Hz, 1H), 6.81 (d, J = 1.79 Hz, 1H), 5.54 (d, J = 10.87 Hz, 1H), 4.37 (dd, J = 6.54, 4.52 Hz, 1H), 4.15 (d, J = 10.85 Hz, 1H),

dx.doi.org/10.1021/ja3125417 | J. Am. Chem. Soc. 2013, 135, 7223−7234

2.98 (s, 3H), 2.81 (s, 3H), 1.70 (dd, J = 15.24, 6.67 Hz, 1H), 1.20 (dd, J = 15.26, 4.43 Hz, 1H), 0.91 (s, 9H). ^{13}C (75 MHz, CD_3OD): 177.03, 169.16, 144.95, 136.94, 135.68, 135.34, 131.25, 130.20, 130.10, 128.88, 128.33, 124.24, 123.43, 112.43, 65.98, 65.14, 60.60, 60.24, 44.23, 38.07, 37.04, 30.97, 29.77. ESI-MS calculated for $C_{25}H_{30}{}^{35}Cl_2N_3O_2$ $[M + H]^+$ = 474.17, Found: 474.50. $[\alpha]_D{}^{25}$ = −132.9° (c = 0.0031, MeCN).

*(2′S,3R,4′R,5′R)-6-Chloro-4′-(3-chlorophenyl)-N-methyl-2′-neopentyl-2-oxospiro[indoline-3,3′-pyrrolidine]-5′-carboxamide (**2b**, TFA salt).* ^{1}H NMR (300 MHz, CD_3OD): 7.63 (d, J = 8.06 Hz, 1H), 7.30−7.14 (m, 4H), 7.12−7.00 (m, 1H), 6.82−6.76 (m, 1H), 5.29 (d, J = 11.24 Hz, 1H), 4.47 (d, J = 6.68 Hz, 1H), 4.16 (d, J = 11.22 Hz, 1H), 2.73 (s, 3H), 1.92 (dd, J = 15.40, 8.39 Hz, 1H), 1.17 (d, J = 16.85 Hz, 1H), 0.90 (s, 9H). ^{13}C (75 MHz, CD_3OD): 177.78, 168.54, 145.38, 137.07, 135.77, 134.60, 131.40, 130.29, 129.48, 128.29, 126.32, 124.24, 124.16, 112.18, 65.11, 64.18, 62.85, 56.95, 43.42, 30.97, 29.66, 26.98. ESI-MS calculated for $C_{24}H_{28}{}^{35}Cl_2N_3O_2$ $[M + H]^+$ = 460.16, Found: 460.48.

*(2′S,3R,4′S,5′R)-6-Chloro-4′-(3-chloro-2-fluorophenyl)-N,N-dimethyl-2′-neopentyl-2-oxospiro[indoline-3,3′-pyrrolidine]-5′-carboxamide (**3b**, TFA salt).* ^{1}H NMR (300 MHz, CD_3OD): 7.68−7.57 (m, 2H), 7.45−7.35 (m, 1H), 7.22−7.10 (m, 2H), 6.84−6.77 (m 1H), 5.68 (d, J = 10.24 Hz, 1H), 4.64 (d, J = 10.24 Hz, 1H), 4.48 (dd, J = 8.20, 1.70 Hz, 1H), 2.98 (s, 3H), 2.80 (s, 3H), 1.89 (dd, J = 15.48, 8.26 Hz, 1H), 1.14 (dd, J = 15.48, 1.67 Hz, 1H), 0.89 (s, 9H). ^{13}C (75 MHz, CD_3OD): 177.96, 168.37, 152.99 (d, J_{C-F} = 253.32 Hz), 145.26, 137.39, 132.82, 128.82, 126.95, 126.70 (d, J_{C-F} = 4.79 Hz), 124.28, 122.09 (d, J_{C-F} = 13.13 Hz), 118.90, 115.11, 112.24, 64.69, 59.97, 42.64, 37.96, 37.03, 31.03, 29.62. ESI-MS calculated for $C_{25}H_{29}{}^{35}Cl_2FN_3O_2$ $[M + H]^+$ = 492.16, Found: 492.46.

*(2′S,3R,4′S,5′R)-6-Chloro-4′-(3-chloro-2-fluorophenyl)-N-methyl-2′-neopentyl-2-oxospiro[indoline-3,3′-pyrrolidine]-5′-carboxamide (**4b**, TFA salt).* ^{1}H NMR (300 MHz, CD_3OD): 7.65−7.55 (m, 2H), 7.40−7.34 (m, 1H), 7.20−7.10 (m, 2H), 6.84−6.80 (m, 1H), 5.26 (d, J = 11.15 Hz, 1H), 4.64 (d, J = 11.19 Hz, 1H), 4.45 (d, J = 7.86 Hz, 1H), 2.74 (s, 3H), 1.87 (dd, J = 15.19, 8.58 Hz, 1H), 1.11 (d, J = 15.21 Hz, 1H), 0.90 (s, 9H). ^{13}C (75 MHz, CD_3OD): 177.75, 168.20, 159.53 (d, J_{C-F} = 248.25 Hz), 145.22, 137.24, 132.59, 128.58, 126.63 (d, J_{C-F} = 5.25 Hz), 124.16, 123.43, 126.66, 122.59 (d, J_{C-F} = 4.05 Hz), 121.54 (d, J_{C-F} = 12.75 Hz), 112.13, 64.49, 64.40, 62.73, 55.34, 43.33, 31.01, 29.58, 27.06. ESI-MS calculated for $C_{24}H_{27}{}^{35}Cl_2FN_3O_2$ $[M + H]^+$ = 478.15, Found: 478.25.

*(2′S,3R,4′S,5′R)-6-Chloro-4′-(3-chloro-2-fluorophenyl)-N-((S)-3,4-dihydroxybutyl)-2′-neopentyl-2-oxospiro[indoline-3,3′-pyrrolidine]-5′-carboxamide (**5b**, TFA salt).* ^{1}H NMR (300 MHz, CD_3OD): 7.60 (d, J = 8.15 Hz, 1H), 7.55 (t, J = 7.12 Hz, 1H), 7.38 (t, J = 7.57 Hz, 1H), 7.20−7.10 (m, 2H), 6.78 (d, J = 1.70 Hz, 1H), 5.27 (d, J = 11.40 Hz, 1H), 4.62 (d, J = 11.40 Hz, 1H), 4.52 (dd, J = 8.33, 1.29 Hz, 1H), 3.45−3.25 (m, 5H), 1.90 (dd, J = 15.46, 8.38 Hz, 1H), 1.64−1.48 (m, 1H), 1.46−1.32 (m, 1H), 1.14 (dd, J = 15.46, 1.34 Hz, 1H), 0.87 (s, 9H). ^{13}C (75 MHz, CD_3OD): 177.77, 167.67, 157.90 (d, J_{C-F} = 251.2 Hz), 145.21, 137.26, 132.67, 128.64, 126.89 (d, J_{C-F} = 1.88 Hz), 126.65 (d, J_{C-F} = 4.89 Hz), 124.17, 123.43, 122.60 (d, J_{C-F} = 19.0 Hz), 121.52 (d, J_{C-F} = 13.0 Hz), 112.14, 70.99, 67.25, 64.45, 62.873, 43.39, 38.26, 33.78, 31.02, 29.57. ESI-MS calculated for $C_{27}H_{33}{}^{35}Cl_2FN_3O_4$ $[M + H]^+$ = 552.18, Found: 552.42. $[\alpha]_D{}^{25}$ = −36.2° (c = 0.0147, MeOH).

*(2′S,3S,4′S,5′R)-6-Chloro-4′-(3-chloro-2-fluorophenyl)-N-((S)-3,4-dihydroxybutyl)-2′-neopentyl-2-oxospiro[indoline-3,3′-pyrrolidine]-5′-carboxamide (**5c**, TFA salt).* ^{1}H NMR (300 MHz, CD_3OD): 8.37 (s, broad, NH), 7.62 (d, J = 8.11 Hz, 1H), 7.50−7.34 (m, 2H), 7.36−7.10 (m, 2H), 6.83 (d, J = 1.83 Hz, 1H), 4.32 (d, J = 12.09 Hz, 1H), 4.24−4.14 (m, 1H), 3.50−3.10 (m, 5H), 1.86−1.72 (m, 2H), 1.58−1.44 (m, 1H), 1.44−1.26 (m, 1H), 0.80 (s, 9H). ESI-MS calculated for $C_{27}H_{33}{}^{35}Cl_2FN_3O_4$ $[M + H]^+$ = 552.18, Found: 552.42.

*(2′R,3R,4′S,5′R)-6-Chloro-4′-(3-chloro-2-fluorophenyl)-N-((S)-3,4-dihydroxybutyl)-2′-neopentyl-2-oxospiro[indoline-3,3′-pyrrolidine]-5′-carboxamide (**5d**, TFA salt).* ^{1}H NMR (300 MHz, CD_3OD): 7.49 (d, J = 8.02 Hz, 1H), 7.36−7.24 (m, 1H), 7.11 (dd, J = 8.09, 1.89 Hz, 1H), 7.06−6.96 (m, 1H), 6.96−6.88 (m, 1H), 6.80 (d, J = 1.88 Hz, 1H), 4.89 (d, J = 11.57 Hz, 1H), 4.46 (d, J = 11.57 Hz, 1H), 4.35−4.25 (m, 1H), 3.56−3.40 (m, 1H), 3.40−3.20 (m, 4H), 1.70−1.40 (m, 3H), 1.10 (dd, J = 14.59, 3.06 Hz, 1H), 0.91 (s, 9H). ESI-MS calculated for $C_{27}H_{33}{}^{35}Cl_2FN_3O_4$ $[M + H]^+$= 552.18, Found: 552.40.

*(2′S,3R,4′S,5′R)-6-Chloro-4′-(3-chloro-2-fluorophenyl)-N-(2-morpholinoethyl)-2′-neopentyl-2-oxospiro[indoline-3,3′-pyrrolidine]-5′-carboxamide (**6b**, TFA salt).* ^{1}H NMR (300 MHz, CD_3OD): 7.66−7.48 (m, 2H), 7.42−7.32 (m, 1H), 7.20−7.10 (m, 2H), 6.78 (d, J = 1.68 Hz, 1H), 5.38 (d, J = 11.48 Hz, 1H), 4.65 (d, J = 11.48 Hz, 1H), 4.52 (d, J = 7.59 Hz, 1H), 4.00−3.70 (m, 4H), 3.70−3.60 (m, 2H), 3.50−3.40 (m, 2H), 3.40−3.10 (m, 4H), 1.97 (dd, J = 15.40, 8.62 Hz, 1H), 1.12 (d, J = 15.40 Hz, 1H), 0.88 (s, 9H). ^{13}C (75 MHz, CD_3OD): 177.73, 169.20, 145.19, 137.15, 132.54, 128.69, 126.84, 126.64 (d, J_{C-F} = 4.80 Hz), 124.11, 123.72, 122.57 (d, J_{C-F} = 13.19 Hz), 121.77 (d, J_{C-F} = 13.19 Hz), 112.06, 65.08, 64.59, 64.32, 62.69, 57.41, 53.70, 48.47, 43.55, 35.61, 31.06, 29.56. ESI-MS calculated for $C_{29}H_{36}{}^{35}Cl_2FN_4O_3$ $[M + H]^+$ = 577.21, Found: 577.48. $[\alpha]_D{}^{25}$ = −24.7° (c = 0.0171, MeOH).

*(2′S,3R,4′S,5′R)-Ethyl 6-chloro-4′-(3-chloro-2-fluorophenyl)-2′-neopentyl-2-oxospiro[indoline-3,3′-pyrrolidine]-5′-carboxylate (**7b**, TFA salt).* ^{1}H NMR (300 MHz, CD_3OD): 7.59 (d, J = 7.41 Hz, 1H), 7.50−7.42 (m, 1H), 7.40−7.32 (m, 1H), 7.17−7.07 (m, 2H), 6.78 (d, J = 1.65 Hz, 1H), 5.61 (d, J = 12.25 Hz, 1H), 4.56 (d, J = 12.25 Hz, 1H), 4.47 (dd, J = 8.50, 1.50 Hz, 1H), 4.25 (dq, J = 10.77, 7.12 Hz, 1H), 4.13 (dq, J = 10.77, 7.12 Hz, 1H), 1.93 (dd, J = 15.39, 8.67 Hz, 1H), 1.34 (dd, J = 15.39, 1.57 Hz, 1H), 1.10 (t, J = 7.12 Hz, 3H), 0.87 (s, 9H). ESI-MS calculated for $C_{25}H_{28}{}^{35}Cl_2FN_2O_3$ $[M + H]^+$ = 493.15, Found: 493.44.

*(2′S,3R,4′S,5′R)-6-Chloro-4′-(3-chloro-2-fluorophenyl)-2′-neopentyl-2-oxospiro[indoline-3,3′-pyrrolidine]-5′-carboxylic acid (**8b**, TFA salt).* ^{1}H NMR (300 MHz, CD_3OD): 7.58−7.42 (m, 2H), 7.36−7.26 (m, 1H), 7.14−7.02 (m, 1H), 6.75 (s, 1H), 5.43 (d, J = 12.00 Hz, 1H), 4.58 (d, J = 11.97 Hz, 1H), 4.35 (d, J = 8.53 Hz, 1H), 1.87 (dd, J = 15.08, 9.31 Hz, 1H), 1.09 (d, J = 15.31 Hz, 1H), 0.85 (s, 9H). ESI-MS calculated for $C_{23}H_{24}{}^{35}Cl_2FN_2O_3$ $[M + H]^+$ = 465.11, Found: 465.38.

*(2′S,3R,4′S,5′R)-6-Chloro-4′-(3-chloro-2-fluorophenyl)-2′-neopentyl-2-oxospiro[indoline-3,3′-pyrrolidine]-5′-carboxamide (**9b**, TFA salt).* ^{1}H NMR (300 MHz, CD_3OD): 7.54−7.44 (m, 2H), 7.36−7.26 (m, 1H), 7.14−7.00 (m, 2H), 6.70 (d, J = 1.76 Hz, 1H), 5.22 (d, J = 11.36 Hz, 1H), 4.50 (d, J = 11.36 Hz, 1H), 4.41 (d, J = 8.23, 1.85 Hz, 1H), 1.81 (dd, J = 15.46, 8.31 Hz, 1H), 1.06 (dd, J = 15.46, 1.90 Hz, 1H), 0.78 (s, 9H). ESI-MS calculated for $C_{23}H_{25}{}^{35}Cl_2FN_3O_2$ $[M + H]^+$ = 464.13, Found: 464.60.

*(2′S,3R,4′R,5′R)-6-Chloro-4′-(3-chlorophenyl)-5-fluoro-N,N-dimethyl-2′-neopentyl-2-oxospiro[indoline-3,3′-pyrrolidine]-5′-carboxamide (**10b**, TFA salt).* ^{1}H NMR (300 MHz, CD_3OD): 7.66 (d, J = 8.49 HZ, 1H), 7.35−7.12 (m, 4H), 6.86 (d, J = 6.02 Hz, 1H), 5.67 (d, J = 10.03 Hz, 1H), 4.41 (dd, J = 8.20, 1.79 Hz, 1H), 4.13 (d, J = 10.03 Hz, 1H), 2.97 (s, 3H), 2.74 (s, 3H), 1.91 (dd, J = 15.46, 8,20 Hz, 1H) 1.17 (dd, J = 15.46, 1.82 Hz, 1H), 0.91 (s, 9H). ^{13}C (75 MHz, CD_3OD):177.80, 168.54, 156.04 (d, J_{C-F} = 243.74 Hz), 141.04, 136.12, 135.16, 131.81, 130.66, 129.73, 128.52, 125.50 (d, J_{C-F} =7.37 Hz), 123.70 (d, J_{C-F} = 19.58 Hz), 114.43 (d, J_{C-F} =25.50 Hz), 113.62, 65.81, 64.45, 60.58, 57.31, 42.59, 38.04, 37.00, 31.04, 29.63. ESI-MS calculated for $C_{25}H_{29}{}^{35}Cl_2FN_3O_2$ $[M + H]^+$ = 492.16, Found: 492.50.

*(2′S,3R,4′R,5′R)-6-Chloro-4′-(3-chlorophenyl)-5-fluoro-N-methyl-2′-neopentyl-2-oxospiro[indoline-3,3′-pyrrolidine]-5′-carboxamide (**11b**, TFA salt).* ^{1}H NMR (300 MHz, CD_3OD): 7.68 (d, J = 8.47 Hz, 1H), 7.32−7.16 (m, 3H), 7.04 (d, J = 7.63 Hz, 1H), 6.85 (d, J = 6.01 Hz, 1H), 5.23 (d, J = 11.21 Hz, 1H), 4.46 (dd, J = 8.23, 1.76 Hz, 1H), 4.13 (d, J = 11.21 Hz, 1H), 2.71 (S, 3H), 1.90 (dd, J = 15.46, 8.23 Hz, 1H), 1.17 (dd, J = 15.48, 1.75 Hz, 1H), 0.89 (s, 9H). ^{13}C (75 MHz, CD_3OD): 177.57, 168.31, 159.98 (d, J_{C-F} = 244.73 Hz), 140.90, 135.98, 134.31, 131.59, 130.56, 129.45, 128.47, 125.84 (d, J_{C-F} = 7.48 Hz), 123.61 (d, J_{C-F} = 19.45 Hz), 114.33 (d, J_{C-F} = 25.29 Hz), 113.57, 65.62, 64.15, 62.93, 57.04, 63.42, 31.01, 29.60, 27.02. ESI-MS calculated for $C_{24}H_{27}{}^{35}Cl_2FN_3O_2$ $[M + H]^+$ = 478.15, Found: 478.46.

*(2′S,3R,4′R,5′R)-6-Chloro-4′-(3-chlorophenyl)-N-((S)-3,4-dihydroxybutyl)-5-fluoro-2′-neopentyl-2-oxospiro[indoline-3,3′-pyrrolidine]-5′-carboxamide (**12b**, TFA salt).* ^{1}H NMR (300 MHz, CD_3OD): 7.68 (d, J = 8.47 Hz, 1H), 7.32−7.17 (m, 3H), 7.12−7.02

dx.doi.org/10.1021/ja3125417 | J. Am. Chem. Soc. 2013, 135, 7223−7234

(m, 1H), 6.85 (d, J = 6.00 Hz, 1H), 5.23 (d, J = 11.28 Hz, 1H), 4.46 (dd, J = 8.41, 1.91 Hz, 1H), 4.10 (d, J = 11.28 Hz, 1H), 3.50−3.20 (m, 5H), 1.90 (dd, J = 15.18, 8.62 Hz, 1H), 1.65−1.47 (m, 1H), 1.47−1.33 (m,1H), 1.18 (d, J = 15.18 Hz,1 H), 0.89 (s, 9H). ^{13}C (75 MHz, CD_3OD): 177.56, 167.81, 155.99 (d, J_{C-F} = 243.27 Hz), 140.87, 135.98, 134.28, 131.63, 130.60, 129.51, 128.60, 125.82 (d, J_{C-F} = 7.39 Hz), 123.58 (d, J_{C-F} = 19.68 Hz), 114.30 (d, J_{C-F} = 25.32 Hz), 113.55, 70.86, 67.23, 65.53, 64.16, 63.07, 57.35, 43.43, 38.15, 33.78, 31.01, 29.57. ESI-MS calculated for $C_{27}H_{33}{}^{35}Cl_2FN_3O_4$ $[M + H]^+$= 552.18, Found: 552.38; $[\alpha]_D{}^{25}$ = 1.1° (c = 0.0334, free amine in MeOH).

*(2′S,3R,4′R,5′R)-6-Chloro-4′-(3-chlorophenyl)-5-fluoro-N-((1r,4R)-4-hydroxycyclohexyl)-2′-neopentyl-2-oxospiro[indoline-3,3′-pyrrolidine]-5′-carboxamide (**13b**, TFA salt).* ^{1}H NMR (300 MHz, CD_3OD): 7.66 (d, J = 8.45 Hz, 1H), 7.30−7.16 (m, 3H), 7.10−7.03 (m, 1H), 6.85 (d, J = 5.98 Hz, 1H), 5.22 (d, J = 11.37 Hz, 1H), 4.46 (dd, J = 8.31, 1.68 Hz, 1H), 4.09 (d, J = 11.37 Hz, 1H), 3.70−3.50 (m, 1H), 3.50−3.39 (m, 1H), 2.00−1.84 (m, 3H), 1.82−1.70 (m, 1H), 1.58−1.46 (m, 1H), 1.40−1.12 (m, 4H), 1.08−0.90 (m, 1H), 0.88 (s, 9H). ^{13}C (75 MHz, CD_3OD): 177.42, 166.80, 155.82 (d, J_{C-F} = 243.61 Hz), 140.67 (d, J_{C-F} = 2.77 Hz), 135.73, 134.18, 131.36, 130.33, 129.44, 128.37, 125.77 (d, J_{C-F} = 7.38 Hz), 123.38 (d, J_{C-F} = 19.54 Hz), 114.06 (d, J_{C-F} = 25.18 Hz), 113.39, 69.97, 65.12, 64.06, 62.94, 57.41, 49.88, 43.37, 34.38, 34.29, 30.98, 30.82, 29.39. ESI-MS calculated for $C_{29}H_{35}{}^{35}Cl_2FN_3O_3$ $[M + H]^+$ = 562.20, Found: 562.36.

*(2′S,3R,4′S,5′R)-6-Chloro-4′-(3-chloro-2-fluorophenyl)-N-(cis-3-hydroxy-3-ethylcyclobutyl)-2′-neopentyl-2-oxospiro[indoline-3,3′-pyrrolidine]-5′-carboxamide (**15b**, MI-888, TFA salt).* ^{1}H NMR (300 MHz, MeOD-d_4): 7.62−7.53 (m, 2H), 7.45−7.35 (m, 1H), 7.20−7.10 (m, 2H), 6.80−6.85 (m, 1H), 5.11 (d, J = 11.07 Hz, 1H), 4.57 (d, J = 11.07 Hz, 1H), 4.40 (d, J = 7.39 Hz, 1H), 4.00−3.80 (m, 1H), 2.50−2.35 (m, 1H), 2.35−2.20 (m, 1H), 2.10−1.90 (m, 1H), 1.90−1.60 (m, 2H), 1.30 (s, 3H), 1.20−1.05 (m, 1H), 0.88 (s, 9H). ^{13}C NMR (75 MHz, MeOD-d_4): 177.85, 167.96, 157.67 (d, J_{C-F} = 249.51 Hz), 144.96, 136.85, 132.22, 128.53, 126.58, 126.34 (d, J_{C-F} = 4.76), 123.91, 123.69, 122.30 (d, J_{C-F} = 18.97 Hz), 122.02 (d, J_{C-F} = 13.10 Hz), 111.84, 67.14, 64.67, 64.53, 62.91, 45.53, 45.47, 43.38, 38.08, 30.84, 29.50, 27.39. ESI-MS calculated for $C_{28}H_{33}{}^{35}Cl_2FN_3O_3$ $[M + H]^+$: 548.19, Found: 548.25. $[\alpha]_D{}^{25}$ = −16.3° (MeOH, c = 0.0284 g/mL).

2. FP-based Protein Binding Assay. The binding affinity of MDM2 inhibitors was determined by an optimized, sensitive and quantitative fluorescence polarization-based (FP-based) binding assay, using a recombinant human His-tagged MDM2 protein (residues 1−118) and a FAM tagged p53-based peptide as the fluorescent probe.

The design of the fluorescent probe was based upon a previously reported high affinity p53-based peptidomimetic compound (5-FAM-βAla-βAla-Phe-Met-Aib-pTyr-(6-Cl-LTrp)-Glu-Ac3c-Leu-Asn-NH_2),[11] termed PMDM6-F. The K_d value of PMDM6-F with the MDM2 protein was determined to be 1.4 ± 0.3 nM by monitoring the total fluorescence polarization of mixtures composed with the fluorescent probe at a fixed concentration and the MDM2 protein with increasing concentrations up to full saturation. Fluorescence polarization values were measured using the Infinite M-1000 plate reader (Tecan U.S., Research Triangle Park, NC) in Microfluor 2 96-well, black, round-bottomed plates (Thermo Scientific).

In the saturation experiments, 1 nM of PMDM6-F and increasing concentrations of proteins were added to each well to a final volume of 125 μL in the assay buffer (100 mM potassium phosphate, pH 7.5, 100 μg/mL bovine γ-globulin, 0.02% sodium azide (Invitrogen), with 0.01% Triton X-100 and 4% DMSO). Plates were incubated at room temperature for 15−30 min with gentle shaking to ensure equilibrium. The polarization values in millipolarization units (mP) were measured at an excitation wavelength of 485 nm and an emission wavelength of 530 nm. Equilibrium dissociation constants (K_d) were then calculated by fitting the sigmoidal dose-dependent FP increases as a function of protein concentrations using Graphpad Prism 5.0 software (Graphpad Software, San Diego, CA).

K_i values of tested compounds were determined in a dose-dependent competitive binding experiment. Mixtures of 5 μL of a solution of the tested compound in different concentrations in DMSO and 120 μL of preincubated protein/fluorescent probe complex with fixed concentrations in the assay buffer (100 mM potassium phosphate, pH 7.5, 100 μg/mL bovine γ-globulin, 0.02% sodium azide, with 0.01% Triton X-100) were added to assay plates and incubated at room temperature with gentle shaking. The incubation time was controlled precisely at 15 min to minimize the influence of the initial isomerization to the binding affinities. Final concentrations of the protein and fluorescent probe in the competitive assays were 10 and 1 nM, respectively, and final DMSO concentration was 4%. Negative controls containing protein/fluorescent probe complex only (equivalent to 0% inhibition), and positive controls containing free fluorescent probe only (equivalent to 100% inhibition), were included in each assay plate. FP values were measured as described above. IC_{50} values were determined by nonlinear regression fitting of the sigmoidal dose-dependent FP decreases as a function of total compound concentrations using Graphpad Prism 5.0 software (Graphpad Software, San Diego, CA). K_i values of tested compounds to the MDM2 protein were calculated using the measured IC_{50} values, the K_d value of the fluorescent probe to the protein, and the concentrations of the protein and fluorescent probe in the competitive assays.[10]

3. Binding Kinetics Studies of 5a, 5b, 5c and 5d and Isomerization Studies in Binding Medium. Aliquots of freshly prepared DMSO stock solutions of compounds **5a**-**5d** were diluted in FP binding assay medium to prepare the aqueous compound incubation solutions in which compound isomerization was taking place. Final compound concentration in the incubation solution was 25 μM, and 5% of DMSO was added to enhance the solubility. These solutions were stored at room temperature for the whole time range of the experiment. 80 μL aliquots of compound solutions were mixed with 20 μL of freshly prepared MDM2/PMDM6-F mixture in the assay plates at different time points. Final concentrations of the protein, fluorescent probe, and DMSO are the same as those in the competitive assays described above. Negative and positive controls were also included in each assay plate. Experimental time was precisely controlled so that each plate was read exactly 10 min after compound solution was pipetted from the incubation solution stock, which typically includes 5 min for plate preparation and 5 min of incubation at room temperature with gentle shaking. mP values were measured and IC_{50} values were determined as described above. Thus, it should be noted that all IC_{50} values presented are values actually obtained 10 min after the incubation times presented.

4. Cell Growth Inhibition Assay. The SJSA-1 osteosarcoma tumor cell line was purchased from the American Type Culture Collection. Cells were seeded in 96-well flat bottom cell culture plates at a density of (3−4) × 10^3 cells/well and grown overnight, then incubated with compounds at different concentrations. The rate of cell growth inhibition after treatment with different concentrations of a compound was determined by assaying with a lactate dehydrogenase-based WST-8 assay (WST-8; Dojindo Molecular Technologies Inc., Gaithersburg, MD). WST-8 solution was added to each well to a final concentration of 10%, and then the plates were incubated at 37 °C for 2−3 h. The absorbance of the samples was measured at 450 nm using a TECAN ULTRA reader. The concentrations of the compounds that inhibited cell growth by 50% (IC_{50}) were calculated by comparing absorbance of the untreated cells with the treated cells.

5. Pharmacodynamic (PD) Study. The SJSA-1 xenograft tumor model was used for PD studies. To develop xenograft tumors, 5 × 10^6 SJSA-1 cancer cells with 50% Matrigel were injected subcutaneously on the dorsal side of SCID mice (Charles River), one tumor per mouse. When xenograft tumors reached a mean of ∼100 mm^3 (70−130 mm^3), two mice were treated with vehicle control (10% PEG400: 3% Cremophor: 87% PBS), 16 mice were treated with a single oral dose of compound **5a** at 200 mg/kg and another 16 mice were treated with a single oral dose of compound **5b** at 200 mg/kg. Mice treated with vehicle control were sacrificed at 6 h and the tumor tissue was harvested for Western blot analysis. Two mice treated with **5b** were sacrificed each time at 1, 3, 6, and 24 h and tumor tissue was harvested. The same schedule was performed on mice treated with **5a**.

6. Western Blotting. For Western blot analysis, tumor cells or tumor tissues were lyzed in ice-cold RIPA buffer: 20 mM Tris-HCl

(pH 7.5), 150 mM NaCl, 1 mM EDTA, 1 mM EGTA, 1% sodium deoxycholate, 2.5 mM sodium pyrophosphate, 1 mM b-glycerophosphate, 1 mM sodium orthovanadate and 1 μg/mL leupeptin. The expressions of indicated proteins in the whole cell lysates were detected by Western blot analysis using the following antibodies: anti-p53 (OP43; Calbiochem), anti-MDM2 (sc-965; Santa Cruz), anti-p21 (556431; BD Biosciences), anti-PARP (9542, Cell Signaling Technology), anticaspase-3 (AAP-113, Stressgen Bioreagents) and HRP-conjugated anti-GAPDH (sc-5778; Santa Cruz).

7. *In vivo* Experiment. For *in vivo* studies, the SJSA-1 xenograft tumor model was used. To develop xenograft tumors, 5×10^6 SJSA-1 cancer cells with 50% Matrigel were injected subcutaneously on the dorsal side of SCID mice (Charles River), one tumor per mouse. When xenograft tumors reached a mean of ~100 mm^3 (70−130 mm^3) the mice were randomized into groups of 8 mice. Vehicle Control (10% PEG400: 3% Cremophor: 87% PBS) was administered p.o. once per day for 14 days. Compound **5a** was administered orally once per day for 14 days at 200 mg/kg and compound **5b** was administered orally once per day for 14 days at 100 and 200 mg/kg. Tumor sizes and animal weights were measured three times per week. Data are represented as mean tumor volumes. Tumor volume (mm^3) = $(A \times B^2)/2$ where A and B are the tumor length and width (in mm), respectively. Statistical analyses were done by two-way ANOVA and unpaired two-tailed t test, using Prism (version 4.0, GraphPad). $P < 0.05$ was considered statistically significant. The same protocol was applied to compounds **15a** and **15b**.

8. Pharmacokinetics of 5a and 5b in Tumor Bearing SCID Mice. The SJSA-1 xenograft tumor model was used for PK studies. To develop xenograft tumors, 5×10^6 SJSA-1 cancer cells with 50% Matrigel were injected subcutaneously on the dorsal side of SCID mice (Charles River), one tumor per mouse. When xenograft tumors reached a mean of ~100 mm^3 (70−130 mm^3), three mice were treated with vehicle control (10% PEG400: 3% Cremophor: 87% PBS), nine mice were treated with a single oral dose of compound **5a** at 100 mg/kg and another nine mice were treated with a single oral dose of compound **5b** at 100 mg/kg. Three mice treated with **5a** were sacrificed each time at 1, 6, and 24 h, and the plasma and the tumor tissue were harvested and frozen at −78 °C immediately. The same schedule was performed on mice treated with **5b**.

The quantitative LC-MS/MS analysis were conducted using an Agilent 1200 HPLC system coupled to an API 3200 mass spectrometer (Applied Biosystems, MDS Sciex Toronto, Canada) equipped with an API electrospray ionization (ESI) source. Aliquots (5 μL) were injected into a reversed-phase column (5 cm × 4.6 mm I.D., packed with 3.5 μm Xbridge C18, Waters). The mobile phase consisted of 0.1% formic acid in water (A) and 0.1% formic acid in acetonitrile (B). The gradient of mobile phase was as follows: 5% B for 0.5 min, 5% to 60% B over 7.5 min, 60% B for an additional 7.5 min, and then immediately set back to 5% B for re-equilibration. The flow rate of the mobile phase was 1.0 mL/min.

Internal standard (150 μL, 100 ng/mL in acetonitrile) was added to 50 μL of previously collected mice plasma or tumor tissue homogenate to precipitate proteins. Five μL of supernatant was injected into the LC-MS/MS instrument. The mass spectrometer was operated at ESI positive ion mode and the detection of the ions was performed in the multiple reaction monitoring (MRM) mode, monitoring the transition of m/z 552.2→m/z 320.1 for **5a** and **5b**. Analyte concentrations in plasma and tumor tissue homogenate were obtained from a calibration curve constructed from the plot of peak area ratio versus concentration. The data was accepted based on the performance of quality control samples (QCs) prepared using SCID mice blank plasma (QCs at three concentrations in duplicate). The calibration range for **5b** was established from 1.0 to 1000 ng/mL in blank SCID mice plasma, and 25 to 10000 ng/g in blank SCID mice tumor tissue homogenate. The calibration range for **5a** was established from 2.0 to 2000 ng/mL in blank SCID mice plasma, and 25.0 to 10000 ng/g in blank SCID mice tumor homogenate.

■ ASSOCIATED CONTENT

Ⓢ Supporting Information

Experimental procedures and characterization data for all new compounds, experimental procedures for isomerization studies, protein binding test, cytotoxicity studies, tumor size measurement, and statistic data of efficacy studies. This material is available free of charge via the Internet at http://pubs.acs.org.

■ AUTHOR INFORMATION

Corresponding Author

shaomeng@umich.edu

Notes

The authors declare the following competing financial interest(s): The compounds described in this paper have been licensed by Ascenta Therapeutics from the University of Michigan, which was sub-licensed to Sanofi. Dr. Shaomeng Wang owns stocks in Ascenta and is a consultant for Ascenta.

■ ACKNOWLEDGMENTS

We are grateful for financial support from the National Cancer Institute, National Institutes of Health (Grants R01CA121279, P50CA06956, and P50CA097248), the University of Michigan Cancer Center (Core Grant P30CA046592), and Ascenta Therapeutics, Inc. and Sanofi S.A. We also thank financial support for J.R.D. provided by NIDA under interagency agreement number ADA12003-001.

■ REFERENCES

(1) (a) Trost, B. M.; Brennan, M. K. *Synthesis* **2009**, *18*, 3003−3025. (b) Galliford, C. V.; Scheidt, K. A. *Angew. Chem., Int. Ed.* **2007**, *46*, 8748−8758. (c) Marti, C.; Carreira, E. M. *Eur. J. Org. Chem.* **2003**, 2209−2219. (d) Bartkovitz, D. J.; Chu, X.-J.; Ding, Q.; Graves, B. J.; Jiang, N.; Zhang, J.; Zhang, Z. PCT patent application WO 2011/067185, 2011 (e) Chen, X.-H.; Wei, Q.; Luo, S.-W.; Xiao, H.; Gong, L.-Z. *J. Am. Chem. Soc.* **2009**, *131*, 13819−13825. (f) Sebahar, P. R.; Williams, R. M. *J. Am. Chem. Soc.* **2000**, *122*, 5666−5667. (g) Nussbaum, F.; Danishefsky, S. J. *Angew. Chem., Int. Ed.* **2000**, *39*, 2175−2178.

(2) Edmondson, S.; Danishefsky, S. J.; Sepp-Lorenzino, L.; Rosen, N. *J. Am. Chem. Soc.* **1999**, *121*, 2147−2155.

(3) Kang, T.-H.; Matsumoto, K.; Tohda, M.; Murakami, Y.; Takayama, H.; Kitajima, M.; Aimi, N.; Watanabe, H. *Eur. J. Pharmacol.* **2002**, *444*, 38−45.

(4) Lo, M.M.-C.; Neumann, C. S.; Nagayama, S.; Perlstein, E. O.; Schreiber, S. L. *J. Am. Chem. Soc.* **2004**, *126*, 16077−16086.

(5) Antonchick, A. P.; Gerding-Reimers, C.; Catarinella, M.; Schürmann, M.; Preut, H.; Ziegler, S.; Rauh, D.; Waldmann, H. *Nat. Chem.* **2010**, *2*, 735−740.

(6) (a) Yu, S.; Qin, D.; Shangary, S.; Chen, J.; Wang, G.; Ding, K.; McEachern, D.; Qiu, S.; Nikolovska-Coleska, Z.; Miller, R.; Kang, S.; Yang, D.; Wang, S. *J. Med. Chem.* **2009**, *52*, 7970−7973. (b) Shangary, S.; Qin, D.; McEachern, D.; Liu, M.; Miller, R. S.; Qiu, S.; Nikolovaska-Coleska, Z.; Ding, K.; Wang, G.; Chen, J.; Bernard, D.; Zhang, J.; Lu, Y.; Gu, Q.; Shah, R. B.; Pienta, K. J.; Ling, X.; Kang, S.; Guo, M.; Sun, Y.; Yang, D.; Wang, S. *Proc. Natl. Acad. Sci. U.S.A.* **2008**, *105*, 3933−3938. (c) Ding, K.; Lu, Y.; Nikolovska-Coleska, Z.; Wang, G.; Qiu, S.; Shangary, S.; Gao, W.; Qin, D.; Stuckey, J.; Krajewski, K.; Roller, P. P.; Wang, S. *J. Med. Chem.* **2006**, *49*, 3432−3435. (d) Ding, K.; Lu, Y.; Nikolovska-Coleska, Z.; Qiu, S.; Ding, Y.; Gao, W.; Stuckey, J.; Krajewski, K.; Roller, P. P.; Tomit, Y.; Parrish, D. A.; Deschamps, J. R.; Wang, S. *J. Am. Chem. Soc.* **2005**, *127*, 10130−10131.

(7) Ding, K.; Wang, G.; Deschamps, J. R.; Rarrish, D. A.; Wang, S. *Tetrahedron Lett.* **2005**, *46*, 5949−5951.

(8) (a) Marti, C.; Carreira, E. M. *Eur. J. Org. Chem.* **2003**, 2209−2219. (b) Laus, G.; Brössner, D.; Senn, G.; Wurst, K. *J. Chem. Soc.,*

Perkin Trans. 2 **1996**, 1931−1936. (c) Finch, N.; Taylor, W. I. *J. Am. Chem. Soc.* **1962**, *84*, 3871−3877.
(9) (a) Wenkert, E.; Udelhofen, J. H.; Bhattacharyya, N. K. *J. Am. Chem. Soc.* **1959**, *81*, 3763−3768. (b) van Tamelen, E. E.; Yardley, J. P.; Miyano, M.; Hinshaw, W. B., Jr. *J. Am. Chem. Soc.* **1969**, *91*, 7333−7341. (c) Seaton, J. C.; Nair, M. D.; Edwards, O. E.; Marion, L. *Can. J. Chem.* **1960**, *40*, 1035−1042.
(10) Nikolovska-Coleska, Z.; Wang, R.; Fang, X.; Pan, H.; Tomita, Y.; Li, P.; Roller, P. P.; Krajewski, K.; Saito, N. G.; Stuckey, J. A.; Wang, S. *Anal. Biochem.* **2004**, *332*, 261−73.
(11) García-Echeverría, C.; Chène, P.; Blommers, M. J. J.; Furet, P. *J. Med. Chem.* **2000**, *43*, 3205−3208.
(12) Zhao, Y.; Yu, S.; Sun, W.; Liu, L.; Kumar, S.; Lu, J.; McEachern, D.; Li, X.; Sun, D.; Wang, S. *J. Med. Chem.* **2013**, in review.
(13) (a) Vassilev, L. T.; Vu, B. T.; Graves, B.; Carvajal, D.; Podlaski, F.; Filipovic, Z.; Kong, N.; Kammlott, U.; Lukacs, C.; Klein, C.; Fotouhi, N.; Liu, E. A. *Science* **2004**, *303*, 844−848. (b) Rew, Y.; Sun, D.; Turiso, F. G. L. D.; Bartberger, M. D.; Beck, H. P.; Canon, J.; Chen, A.; Chow, D.; Deignan, J.; Fox, B. M.; Huang, X.; Jiang, M.; Jiao, X.; Jin, L.; Kayser, F.; Kopecky, D.; Li, Y.; Lo, M. C.; Long, A.; Michelsen, K.; Oliner, J. D.; Osgood, T.; Ragains, M.; Saiki, A. Y.; Schneider, S.; Toteva, M.; Yakowec, P.; Yan, X.; Ye, Q.; Yu, D.; Zhao, X.; Zhou, J.; Medina, J. C.; Olson, S. J. *Med. Chem.* **2012**, *55*, 4936−4954.